An Aphid-Transmitted Virus Reduces the Host Plant Response to Its Vector to Promote Its Transmission

Célia Krieger, David Halter, Raymonde Baltenweck, Valérie Cognat, Sylvaine Boissinot, Alessandra Maia-Grondard, Monique Erdinger, Florent Bogaert, Elodie Pichon, Philippe Hugueney, et al.

Phytopathology®

An aphid-transmitted virus reduces the host plant response to its vector to promote its transmission

Journal:	*Phytopathology*
Manuscript ID	PHYTO-12-22-0454-FI.R3
Manuscript Type:	Focus Issue
Date Submitted by the Author:	10-Apr-2023
Complete List of Authors:	Krieger, Célia; IBMP CNRS - Strasbourg University Halter, David; Université de Strasbourg, INRAE, SVQV UMR-A1131 28 rue de Herrlisheim Colmar, Grand Est, FR 68000 Baltenweck, Raymonde; Université de Strasbourg, INRAE, SVQV UMR-A1131 Cognat, Valérie; IBMP CNRS - Strasbourg University Boissinot, Sylvaine; Université de Strasbourg, INRAE, SVQV UMR-A1131 28 rue de Herrlisheim Colmar, Grand Est, FR 68000 Maia-Grondard, Alessandra; Université de Strasbourg, INRAE, SVQV UMR-A1131 Erdinger, Monique; Université de Strasbourg, INRAE, SVQV UMR-A1131 28 rue de Herrlisheim Colmar, Grand Est, FR 68000 Bogaert, Florent; Université de Strasbourg, INRAE, SVQV UMR-A1131 28 rue de Herrlisheim Colmar, Grand Est, FR 68000 Pichon, Elodie; Université de Strasbourg, INRAE, SVQV UMR-A1131 28 rue de Herrlisheim Colmar, Grand Est, FR 68000 Hugueney, Philippe; Université de Strasbourg, INRAE, SVQV UMR-A1131 Brault, Veronique; INRA, UMR SVQV Ziegler, Veronique; IBMP CNRS - Strasbourg University
Keywords:	Virology, Molecular, Metabolomics, Host Parasite Interactions, Genomics

An aphid-transmitted virus reduces the host plant response to its vector to promote its transmission

Célia Krieger [a,1], David Halter [b,c,1], Raymonde Baltenweck [b], Valérie Cognat [a], Sylvaine Boissinot [b], Alessandra Maia-Grondard [b], Monique Erdinger [b], Florent Bogaert [b], Elodie Pichon [b], Philippe Hugueney [b], Véronique Brault [b,2], Véronique Ziegler-Graff [a,2]

[a] Institut de biologie moléculaire des plantes, CNRS, Université de Strasbourg, 67084 Strasbourg, France.

[b] INRAE, Université de Strasbourg, SVQV UMR1131, 68000 Colmar, France

[1] These authors contributed equally to this work.

[2]Corresponding authors: V. Brault; E-mail: veronique.brault@inrae.fr

V. Ziegler-Graff; E-mail: veronique.ziegler-graff@ibmp-cnrs.unistra.fr

Keywords: *Arabidopsis thaliana*, *Myzus persicae*, polerovirus, turnip yellows virus, transcriptomics, metabolomics, vector transmission

Funding: This research was financed by the French National Agency for Research (ANR) in the frame of VIRAPHIPLANT (ANR-14-CE19-0010-01) (CK, DH, FB, EP).

Abstract

The success of virus transmission by vectors relies on intricate trophic interactions between three partners, the host plant, the virus and the vector. ~~Even if~~ Despite numerous studies ~~have~~ that showed~~n~~ the capacity of plant viruses to manipulate their ~~plant~~ host plant to the benefit of their vector, and potentially of their transmission, the molecular mechanisms sustaining this phenomenon has not yet been extensively analyzed at the molecular level. In this study, we focused on the deregulations induced in *Arabidopsis thaliana* by an aphid vector that were alleviated when the plants were infected with turnip

yellows virus (TuYV), a polerovirus strictly transmitted by aphid in a circulative and non-propagative mode. By setting up an experimental design mimicking the natural conditions for virus transmission, we analyzed the deregulations in plants infected with TuYV and infested with aphids by a dual transcriptomic and a metabolomic approach. We observed that the virus infection alleviated most of the gene deregulations induced by the aphid in a non-infected plant at both time points analyzed (6 and 72 h) with a more pronounced effect at the later time point of infestation. The metabolic composition of the infected and infested plants was altered in a way that could be beneficial for the vector and the virus transmission. Importantly, these substantial modifications observed in infected and infested plants correlated with a higher TuYV transmission efficiency. This study revealed the capacity of TuYV to alter the plant nutritive content and the defense reaction against the aphid vector to promote the viral transmission.

Introduction

As their host plants are immobile, the vast majority of phytoviruses rely on insect vectors for their dispersal among hosts and their survival ((Whitfield et al. 2015); (Bragard et al. 2013)). Different strategies of viral transmission have been described allowing a virus to be recognized and transported by its vector in a non-persistent, semi-persistent or persistent mode depending on the retention time and the virus location in the insect (Whitfield et al. 2015). ~~Persistent~~ Among persistently-transmitted viruses ~~encompass viruses that~~some replicate in insect tissues (propagative mode) and ~~viruses that~~others only circulate in the insect body without replicating ~~there~~ (non-propagative mode). For these viruses, insects are more than simple transport devices as sophisticated and highly specific relationships have evolved between viral proteins and their vector partners ((Brault et al. 2010); (Dietzgen et al. 2016)).

Plant virus-insect relationships display additional complexities. A growing body of evidence shows that virus infection influences vector orientation, settling and feeding behavior, and impacts vector performance through host plant physiological alterations ((Mauck et al. 2012); (Mauck et al. 2018); (Dáder et al. 2017)). Such changes are mostly indirect as the virus impacts the physiology of the shared host plant, but direct effects on the vector behavior following virus acquisition and retention in the insect have also

been reported with consequences at ~~an~~ epidemiological and ecological levels ((Sisterson 2008); (Mauck 2016); (Eigenbrode et al. 2018); (Carr et al. 2020); (Cunniffe et al. 2021); (Marmonier et al. 2022)). Plant metabolism alterations and defensive signaling pathways triggered by viruses can modify vector behavior with consequences on viral transmission ((Mauck et al. 2019); (Bera et al. 2020); (Mishra et al. 2012); (Wamonje et al. 2020); (Hu et al. 2020)).

Importantly, the virus-induced plant changes are not simply side effects of the infection but are under genetic control of the virus (reviewed in (Carr et al. 2018); (Mauck et al. 2019)). Several virus-encoded silencing suppressor proteins of persistently- and non-persistently vector-transmitted viruses ~~able to~~can inhibit the plant RNA silencing defense pathway, ~~have been shown to~~and in doing so, modulate the vector preference or performance, and subsequently, transmission ((Mauck et al. 2019); (Wu and Ye 2020) ; (Ziegler-Graff 2020)). A remarkable recent example is a plant virus satellite of the non-persistently aphid-transmitted cucumber mosaic virus (CMV) that promotes the formation of winged aphids that can enable virus spread (Jayasinghe et al. 2021). Interestingly, virus-induced changes affecting vector behavior were also observed at the plant cellular level. Bak et al. (2017) demonstrated that the NIa-Pro protein encoded by the non-persistent turnip mosaic virus (TuMV) was relocalized to the vacuole in response to the presence of the aphid vector. T~~, and t~~his dynamic localization modification was responsible for higher vector performance and increased viral transmission rate. Another example is the semi-persistent cauliflower mosaic virus that responds to the aphid vector punctures by relocalizing the viral components of the transmissible complex (*i.e.*, the viral transmission factor P2 and the viral particles), onto microtubules to facilitate virus acquisition and transmission by the vector (Martinière et al. 2013). This particular “transmission activation” phenomenon has since then also been observed for TuMV (Berthelot et al. 2019).

In this work, we investigated the global response of plants exposed to both a plant virus and its vector, in conditions resembling natural settings for virus uptake by the vector., ~~and~~ W~~w~~e then compared these deregulations with those of plants that were treated with single pests. We aimed to decipher the contribution of the viral infection to aphid-induced changes on the plant physiology that could be

conducive to vector performance and viral transmission. The pathosystem consisted of the phloem-limited and persistently-transmitted turnip yellows virus (TuYV, *Solemoviridae* family, *Polerovirus* genus), the *Myzus persicae* aphid vector and the compatible host plant *Arabidopsis thaliana*. We undertook a high throughput analysis of the transcriptional response pattern of viral-infected plants that were infested by aphids for ~~two~~ either 6 or 72 hours, ~~time points~~ and of plants that were only aphid-infested or only virus-infected. A non-targeted metabolomic analysis was performed in parallel on the same plants to find related deregulated pathways. Finally, virus transmission experiments were conducted with similar aphid infestations to correlate our findings at the molecular level to ~~the~~ consequences on ~~the insects regarding~~ TuYV transmission.

Material and Methods

Plants, aphids and aphid infestations

Arabidopsis thaliana Col-0 were grown in a growth chamber under 20 ±1 °C and 10 h photoperiod under fluorescent lamps. The *Myzus persicae* (Sulzer) (Hemiptera: Aphididae) clone collected in 1974 on sugar beet was since then reared on pepper (*Capsicum annuum*) at 20 °C with a 16 h photoperiod. For the preliminary metabolomic experiment, non-infected *A. thaliana* Col-0 were infested with 30 non-viruliferous wingless *M. persicae* for 6, 24, 48, 72 and 96 h.

TuYV infection and aphid infestation of Arabidopsis thaliana plants used in the high throughput experiments and the transmission assays

A. rabidopsis thaliana Col-0 were inoculated three weeks post-sowing using viruliferous *M. persicae*. Non-viruliferous aphids were fed on an artificial medium (Bruyère et al. 1997) containing purified TuYV at a concentration of 100 ng/µL and prepared as described in (J. M. van den Heuvel 1991). After 24 h of acquisition, two aphids were transferred onto each Col-0 plant for 72 h. Aphids were then manually gently eliminated with a soft brush to avoid any effect of an insecticide treatment on the plant physiology and

the plants were grown for three more weeks. Mock non-inoculated plants were treated similarly without addition of virus in the artificial medium.

Thirty ~~apterous~~ non-viruliferous aphids of mixed developmental stages were then deposited on TuYV-infected plants and on control ~~non-infected~~mock-inoculated plants for 6 h or 72 h (see Suppl Table 1 for details on the number of treated plants). The entire aerial tissues ~~of the plants~~ were harvested ~~individually~~ on individual plants at three time points (0 h, 6 h and 72 h) and flash-frozen in liquid nitrogen, split in three batches to be processed for virus detection by DAS-ELISA (enzyme-linked immunosorbent assay) (Clark and Adams 1977) with a rabbit polyclonal antiserum raised against TuYV (LOEWE, France), and for transcriptomic and metabolomic analyses.

RNA sample preparation for the transcriptomic and data processing

Total RNA from leaf tissues of individual plants were extracted using Tri Reagent® (Sigma) following the manufacturer's recommendations and treated with RNAse-free DNase I (Thermo Scientific, Inc.) to remove any DNA contamination. RNA samples were quantified and sample purity was verified using a Nanodrop spectrophotometer (Thermo Fischer Scientific). Sample purity was considered as acceptable with 260/280 nm and 260/230 nm ratios of 1.8-2.0. Then, total RNA from three to four plants were pooled with equal amounts of nucleic acids of each plant and quantified using the Qubit fluorometer and Qubit RNA BR Assay kit (Thermo Scientific, Inc.). Three replicates were set up for each condition (Suppl. Table S1). RNA integrity was further checked with the 2100 Bioanalyzer™ capillary electrophoresis system (Agilent Technologies, Palo Alto, CA) using the Plant RNA 6000 Nano kit. Three µg of total RNA per sample was send to Fasteris (http://www.fasteris.com, Switzerland) to generate strand-specific RNA-seq libraries. Following quality control, the libraries were sequenced (paired-end 2 × 75 pb) on the Illumina HiSeq 4000 platform. Sequence data was deposited onto GEO under the submission number GSE218846.

Between 13 and 23 million reads were obtained per library. Initial quality assessment of raw RNA-seq data was performed with FastQC version 0.11.2 (Andrews 2010). Duplicated paired reads were removed from each library using FastUniq version 1.1 (Xu et al. 2012). Remaining reads were mapped against *A. thaliana*

genome TAIR10 using HiSAT2 version 2.0.5 (Kim et al. 2015) (Suppl. Table ~~S1~~S2). The count of overlapping reads with genes was assessed with HTSeq-count version 0.6.1 (Anders et al. 2015) using intersection-nonempty option. Differential analysis of count data was realized with DESeq2 version 1.14.1 (Love et al. 2014) with pre-filtering to keep only genes that have a least one read. The conditions were compared two by two, and genes with $|\log_2 FC| \geq 0.75$ and corresponding *p*-value less than 0.05 were considered as statistically deregulated.

The deregulated genes identified in the five differential analyses (A, B, C, F and G) were subjected to hierarchical clustering analysis using the TIGR MultiExperiment Viewer (MeV) software (Howe et al. 2010). A first step of hierarchical clustering was performed using the non-parametric Kendall's tau similarity metric and single linkage as the aggregation method. Six branches were extracted which correspond to differentially expressed genes (DEGs) specifically deregulated by the virus, ~~specifically deregulated~~ by aphids in non-infected plants, ~~and~~ or ~~specifically deregulated~~ by aphids in infected plants. Then, a second step of hierarchical clustering was achieved with all DEGs belonging to the six branches with Pearson correlation distance matrix and average linkage as the aggregation method. Six clusters were obtained and extracted to realize a final step of hierarchical clustering using Euclidean Correlation similarity metric and average linkage as the aggregation method.

DEGs were analyzed using MapMan software (MapMan v 3.6.0 (Thimm et al. 2004). This tool is specifically designed for plant-specific pathways and is composed of a scavenger gene ontology in which genes are assigned into largely and non-redundant and hierarchically organized BINs (34) divided into subBINs. Three functional categories (gluconeogenesis, tricarboxylic acid (TCA) and polyamine metabolism) were not or poorly represented (0 or 1 DEG/condition) and were therefore not considered in the figure.

Comparison between the data and transcriptomic data from the literature

A review of public transcriptomic data was carried out. We selected experiments analyzing *M. persicae* infestation in similar conditions to compare the data. As these data resulted from microarray assays, they were retrieved and reanalyzed using our former significance standards ($\log_2$FC and p-value). The raw data

were downloaded from ArrayExpress (https://www.ebi.ac.uk/biostudies/arrayexpress/) : E-MTAB-3223 (Jaouannet et al. 2015) and GEO (https://www.ncbi.nlm.nih.gov/geo/): GSE40924 (Bricchi et al. 2012) and GSE5525 (De Vos et al. 2005). The single channel Agilent microarray E-MTAB-3223 was analyzed with R using the limma package (Ritchie et al. 2015). The 6 h dataset was compared to the wild type (WT) dataset. The data were normalized according the quantile normalization method and the p-value adjusted by Bonferroni & Hochberg method. The two channels Agilent microarray GSE40924 was analyzed with R using the limma package. The 5 h versus WT dataset was normalized according to the loess method and the p-value adjusted by Bonferroni & Hochberg method. The single channel Affymetrix microarray GSE5525 was analyzed with R using the affy and limma packages. The 72 h versus WT dataset was background corrected and normalized using quantile normalization.

Validation of gene expression by ~~q~~RT-qPCR

Twelve differentially expressed genes (identified by RNA-seq) were selected for validation using ~~q~~RT-qPCR. One µg of total RNA from *A. thaliana* was denatured and reversed-transcribed with 0.5 µg oligo $(dT)_{18}$ (Thermo Scientific, Inc.), 0.2 µg of random hexamer (Thermo Scientific, Inc.) primers, 1 mM of dNTP, 4 µL of 5X reaction buffer, 0.5 µl RNAse OUT (Invitrogen), 1 µL of RevertAid^{TM} H minus Reverse Transcriptase (Thermo Scientific, Inc.), in a final volume of 20 µL by incubating for 1 h at 42°C followed by 10 min at 70°C. Real-time PCR was performed on 10 ng cDNA using SYBR Green I Master reagent (Roche) according to the manufacturer's recommendations in a LightCycler 480 apparatus (Roche Life Science, Penzberd, Germany) with gene-specific primers listed in Supplementary Table 2. Three technical replicates were used to calculate the relative gene expression levels by means of the linear regression of efficiency method using LinRegPCR software (version 7.4) and normalized to the internal reference genes EF1α (AT5G60390) and TIP41 (AT4G34270).

Metabolomic analyses and data processing

A preliminary experiment of non-targeted metabolomic analysis was performed on non-infected *A. thaliana* Col-0 infested with non-viruliferous *M. persicae*. Then, two independent experiments including all conditions described in Fig. 2 were performed, with a minimum of ~~nine~~ six biological replicates for each condition and time point (Suppl. Table 1).

For metabolomic analyses, *A. thaliana* leaf~~ve~~ samples were ground in liquid nitrogen and a fraction of 100 mg was added to 500 µL of extraction buffer (70 %/30 % MeOH/H_2O supplemented with 1 µg/ml of apigenin as internal standard). The homogenate was vortexed, heated 5 min at 80 °C in a water bath to inactivate myrosinases, ultrasonicated in a water bath during 5 min and centrifuged twice 5 min at 4 °C at 16 000 g. The final supernatant was collected and stored at -80 °C until processed.

The metabolic analyses were performed using a Dionex Ultimate 3000 UHPLC system (Thermo Fisher Scientific, San Jose, USA). The chromatographic separation was performed on a CSH C18 column (100 mm x 2.1 mm, 1.7 µm particle size; Waters, Wexford, Ireland) maintained at 25 °C with elution at 0.4 mL/min. Eluents used were as follows: eluent A: water/formic acid (0.1 %, v/v); eluent B: acetonitrile/formic acid (0.1 %, v/v). The separation program used was as follows: 98 % eluent A under the initial conditions, 98 % to 55 % eluent A in 6 min, 55 % to 0 % eluent A in 0.5 min and isocratic with 0 % eluent A during 2 min. One µL of the sample volume was injected. The UHPLC system was coupled to an Exactive Orbitrap mass spectrometer (Thermo Fischer Scientific) equipped with an Electrospray Ionization (ESI) source operating in positive mode and negative mode. Parameters were set at 300 °C for ion transfer capillary temperature. Nebulization with nitrogen sheath gas and auxiliary gas were maintained at 40 and 10 arbitrary units, respectively. The spectra were acquired within the m/z mass range of 100–1,200 atomic mass units (amu), using a resolution of 50,000 at m/z 200 amu. The system was calibrated internally using dibutylphthalate as lock mass at m/z 279.1591, giving a mass accuracy lower than 1 ppm in positive mode. The instruments were controlled using the Xcalibur software and data was processed using the XCMS software package (Smith et al., 2006). Raw data were converted to the mzXML format using MSconvert before analysis. Settings of the xcmsSet function of XCMS were as follows: method = “centWave”, ppm = 2, noise = 30000, mzdiff = 0.001, prefilter = c(5,15000), snthresh = 6, peakwidth = c(6,35). Peaks were aligned using the

obiwarp function using the followings settings of the function group.density: bw = 10, mzwid = 0.0025. This allowed the alignment of 1,967 and 4,678 ions in the negative and positive mode, respectively. Metabolic features were annotated automatically by XCMS as MxxxTyyy, where xxx is the m/z and yyy the retention time in seconds.

For differential analyses, the $\log_2$(FC) was calculated on the means of the samples of both experiments. Statistical analyses were performed using the Tukey's Honest Significant Difference method followed by a false discovery rate (FDR) correction using the Benjamini-Hochberg procedure. Metabolites of interest were considered differentially accumulated when the false discovery rate was below 5 % (FDR < 0.05).

Quantification of viral RNA by qRT-qPCR

To measure TuYV accumulation in infected plants, total RNA from leaf tissues was extracted using the RNeasy minikit (Qiagen, Hilden Germany) following the manufacturer's recommendations and the concentration was measured by quantification at 260 nm (Nanodrop 2000; Thermo Fischer Scientific). 0.2 µg of total RNA extracted from plant was reversed-transcribed using the reverse primer (5' GGAGACGAACTCCAAAATGAC 3') hybridizing to the major coat protein sequence and the Moloney murine leukemia virus (MMLV) reverse transcriptase (Promega corporation). The PCR was performed using the iTaq™ Universal SYBR® Green Supermix (Biorad) according to the manufacturer's recommendations with the aforementioned reverse primer and the forward primer (5' AAGACAATCTCGCGGGAAG 3'). PCR runs were performed on a CFX96 Touch™ Real-Time PCR Detection System apparatus. Serial 10-fold dilutions of TuYV-cDNA (from 10E+08 to 10E+03 copies of viral cDNA/µL) prepared from 100 ng of viral RNA extracted from purified TuYV particles were used to establish standard curves for each plate. The data were analyzed using the CFX Manager Version 3.0.1224.1015 software.

Results

Analysis of Arabidopsis global metabolic response to non-viruliferous aphids over time

To investigate the global dynamic metabolomic changes in *A. thaliana* Col-0 infested by aphids, we first performed a non-targeted metabolomic analysis on non-infected plants that were infested by non-viruliferous *M. persicae* for different time laps (6 h, 24 h, 48 h, 72 h and 96 h). We observed that among the total 1376 ions detected in the negative mode of Liquid Chromatography-Mass Spectrometry (LC-MS), 259 accumulated differentially in at least one condition (Fig. 1). Moreover, the pattern of these differentially accumulated metabolites (DAM) varied remarkably over the time course and reflected a dynamic plant response to aphids. For instance, most deregulations occurring during the two first days of aphid infestation (6, 24 and 48 h) were transient and did not persist after 72 h whereas the metabolite profiles at 72 h and 96 h looked more similar (Fig. 1). This indicates that aphids induce waves of metabolic changes in plants, depending on the infestation time. ~~These observations are in agreement with the results by (Tzin et al. 2015) who found a dynamic shift in plant responses to aphid feeding between the first hours of infestation by the aphid *Rhopalosiphum maidis* and later time points (after 48h) in maize. Such metabolic deregulations in non-infected *A. thaliana* plants are likely to be affected by additional biotic stresses, like the infection by an aphid-transmitted virus.~~ We ~~therefore~~ selected two time points with contrasted, and not overlapping metabolite deregulations (6 h and 72 h post aphid-infestation), to investigate at the metabolomic and transcriptomic levels modifications of the plant response to aphids in presence or absence of the polerovirus TuYV.

Changes in plant transcriptomic response to aphids upon TuYV infection

The experimental set up designed to decipher the plant response to aphid infestation upon viral infection is ~~described~~ outlined in Fig. 2. ~~*A. thaliana* Col-0 were first inoculated with TuYV-viruliferous, or non-viruliferous aphids that were thereafter manually removed following a 72 h-inoculation period. Three weeks later, non-viruliferous aphids were placed on TuYV- or mock-inoculated plants for 6 h or 72 h (30 aphids per plant) to trigger the plant response to aphids in a viral or a non-viral context. The aerial plant tissues were then collected and each plant extract was split into three pools to be first processed for virus~~

~~detection (by DAS-ELISA), before transcriptomic or metabolomic analyses. Three replicates were generated and processed for transcriptomic analysis (see Material and Methods).~~

The transcriptomic data obtained in the different conditions were first compared with those of the control, mock-inoculated and non-infested plants (Mock-0 h aphids; Fig. 2, sample 2; Fig. 3A, conditions A-E) and then filtered using the significance criteria of FDR ≤ 0.05 and $|\log_2(FC)| \geq 0.75$. TuYV infection triggered the deregulation of 1231 genes with 505 up-regulated and 726 down-regulated genes (Fig. 3B, condition A). Aphid-infestation induced the deregulation of 3434 and 2693 genes after 6 h and 72 h of aphid infestation respectively (Fig. 3B, conditions B and C). When plants were infected by TuYV and infested with aphids, a higher number of DEG was observed in both conditions, 5130 and 4207 DEG at 6 h and 72 h respectively (Fig. 3B, conditions D and E). The number of genes deregulated in plants subjected to both pests (virus and aphid) compared to mock-inoculated plants (Fig. 3B, condition D and E) was close to the sum of the DEG observed in plants submitted to virus infection and those of plants submitted to aphid infestation (Fig. 3B, conditions A + B for 6 h or A + C for 72 h).

To confirm the gene expression data obtained by RNA-seq, we evaluated by ~~q~~RT-qPCR the deregulation of eleven genes that were found similarly altered (up- or down-regulated) in all conditions and one gene (AT1G76790) which expression varied in both orientations depending on the conditions (Fig. 4A). RNA samples from two independent experiments were tested: those from the experiment used in the transcriptomic study and those from another experiment performed in similar conditions. Figure 4A~~,~~ shows that the same trend of expression was observed when transcript accumulations were measured by ~~q~~RT-qPCR (green and yellow bars representing the two biological repeats), or by RNA-seq (blue bars), with a significant statistical correlation (Fig. 4B). The close gene expression patterns observed between the two techniques (RNA-seq and ~~q~~RT-qPCR) confirm the reliability and quality of the transcriptomic data.

The objective of our study was to specifically investigate the plant response induced by aphids in mock- and virus-infected conditions. We therefore normalized the data obtained in doubled challenged plants with those of TuYV-infected plants. Strikingly, this analysis led to a drastic reduction of the DEG numbers, 1490 and 190 respectively at 6 h and 72 h (Fig. 3B, conditions F and G), compared to the 3434 and 2693

DEG when the plants were only challenged by aphids during similar times (Fig. 3B, conditions B and C). The reduction of the DEG number observed in the doubled treated plants was particularly stressed at 72 h, highlighting a decrease of 93.7% of DEG compared to plants similarly infested by aphids but without viral infection. Venn diagrams (Suppl. Fig. 1) ~~indicated~~ showed the common DEG between mock and infected conditions upon both aphid infestation times. These results underpin that the Arabidopsis response to *M. persicae* infestation at the transcriptional level differs considerably according to the viral infectious status of the plant and suggest that TuYV infection can impact the transcription profile of genes normally deregulated by aphid infestation.

Comparison of our expression profiles of aphid-infested Arabidopsis with those of the literature

Before further investigations on the gene deregulation in the different conditions described, we compared our data in conditions B and C (aphid-deregulated genes) with data in the literature from similar experiments performed on *A. thaliana* Col-0 infested by *M. persicae*. The closest experiments that generated transcriptomic data for early time points of aphid infestation were those of Bricchi et al. (2012) and of Jaouannet et al. (2015) and, for later times, the experiments performed by De Vos et al. (2005). ~~As these data resulted from microarray assays, they were first retrieved and reanalyzed as indicated in Material and Methods using our former significance standards (log_2FC and p-value).~~ We ~~then~~ compared the DEG of these studies with our corresponding analyses. After 5 or 6 h of aphid infestation, 31 common DEG were retrieved (Suppl. Fig. 2; Suppl. Table ~~3~~4). More common DEG were obtained when the data of Bricchi et al. (2012) were compared to ours, highlighting 419 common DEG compared to 96 common DEG between Jaouannet's data and ours. In summary for the early aphid treatment, we obtained 484 DEG common between our data and either one of the two reports, 197 up-regulated and 287 down-regulated (Suppl. Fig. 2). By comparing the data obtained after 72 h post-aphid infestation (our data and those of (De Vos et al. 2005), 661 common DEG were found, 249 up-regulated and 412 down-regulated (Suppl. Fig. 2). Taking into account that these experiments were performed in other laboratories with different biological variables (other *M. persicae* clones, other plant species and aphid growing conditions) and

different gene expression profiling technologies (RNA-seq versus microarrays), these results strongly support our data. We further analyzed the enrichment of GO terms by DAVIDavid functional annotation tool (Huang et al. 2007) among the common DEG according to the time of aphid infestation. Early down-regulated genes were mainly enriched in jasmonic acid, wounding and abscisic acid responsive genes, while up-regulated genes belonged to genes of thepathways for chitin metabolism, the general and bacterial defense responses (Suppl. Fig. 3A and 3B). After 72 h aphid infestation, down-regulated genes were enriched in genes for those involved in responsesding to water deprivation, abscisic acid and wounding. ,A while auxin-responsive genes and genes involved in development andal growth were more represented upon within the up-regulated genes group (Suppl. Fig. 3C and 3D).

Profiling the genes specifically deregulated upon single aphid infestation or dual aphid and TuYV challenge

From our data, we further explored the signatures that were specifically triggered by aphids in plants only infested (Fig. 3A, conditions B and C) or infested and infected (Fig. 3A conditions F and G). To this aim, we performed a hierarchical clustering analysis using the TIGR MultiExperiment Viewer (MeV). Six clusters were extracted from the 5488 DEG found in conditions B, C, F and G. Clusters 1, 2 and 3 correspond to genes specifically deregulated by aphids in non-infected plants either at both 6 h and 72 h, or at each time point respectively, and that were not affected in plants only infested (Fig. 5). Clusters 4, 5 and 6 represent 348 DEG (9.8%) specifically deregulated by aphids in TuYV-infected plants either at both 6 h and 72 h, or at each time point respectively (Fig. 5). Genes that were found deregulated in any other conditions (e.g. at 6 h aphid infestation and 6 h aphid and TuYV treatment) were discarded from this analysis (1943 in total). Clusters 1, 2 and 3 gathered 3197 genes (90.2% of the 3545 total DEG considered here) deregulated by aphids only and that were not deregulated when the virus was present. This clustering emphasizes that TuYV infection can drastically reduce the number of aphid-induced gene deregulations in Arabidopsis (in double-treated plants) and thus hinders a significant number of host gene deregulations, specifically triggered in plants colonized by aphids only.

We then proceeded with a functional annotation of the DEG of the clusters presented in Fig. 5, using MapMan software (Thimm et al. 2004). The DEG in single aphid-infested plants or in double aphid- and TuYV-treated plants (6 h and 72 h) were assigned to one of the 34 different bin code ontologies indexed for *A. thaliana* (Fig. 6). The major bin code ontologies present in the aphid-only treated plant conditions were “RNA processing/transcription/binding” and “proteins” at both time points (Fig. 6, bars at the left, in yellow (6 h), red (72 h) and orange for the genes found at both time points). In particular, 61% and 70% of the genes in the “RNA processing/transcription/binding” category encode transcription factors at 6 h and 72 h of aphid post-infestation respectively and 42% of the genes found in the category “protein” were related to protein degradation processes whatever the time of aphid infestation. Genes belonging to categories like “stress", “peroxidases/gluthathion-S-transferases”, “signaling”, “cell cycle” and “transport” were also highly represented. Genes deregulated in plants treated with both TuYV and aphids fit into similar categories but were considerably less abundant (Fig. 6, bars at the right with the same scale, light green (6 h), dark green (72 h) and intermediate green for the genes found at both time points). These observations highlight the broad impact of TuYV on the transcriptional response specific to plants infested by aphids.

To examine whether there is a specific trend in the deregulations triggered by both pests, ~~treatments~~ we considered the sum of repressed and induced DEG in each GO categories. In plants infested with aphids only, the ratio of repressed genes versus induced genes was significantly higher in the categories “amino acid metabolism”, “secondary metabolism” and “DNA” (Suppl. Fig. 4A). The categories “RNA processing”, “protein” and “cell cycle” contained about twice as much repressed DEG than induced DEG. Among the categories displaying more induced DEG, “cell wall” and “lipid metabolism” categories are the most represented. In plants challenged with both aphids and TuYV, the ratio of repressed versus induced genes was particularly represented in the “photosynthesis”, “glycolysis”, “secondary metabolism”, “signaling”, “microRNA” and “development” categories (Suppl. Fig. 4B). Conversely, a few categories displayed only induced genes like “major CHO metabolism” and “fermentation”.

We also examined the genes encoding transcription factors (TFs) that were differentially expressed in the four experimental conditions (B, C, F and G in Fig. 3A) by clustering them according to their family and their trend of deregulation. Globally, Fig. 7 illustrates the massive difference in the number of TF DEG in plants only infested by aphids (conditions B and C) and those in plants infected by TuYV and aphid infested (conditions F and G). For instance, up to 20 deregulated TF genes were found for the AP2/ERF family in condition C (Fig. 7, 72 h aphids) while, in similar conditions, the presence of the virus led to only one DEG (Fig. 7, condition G, 72 h aphids). A closer look at aphid-infested plants showed that some DEG belonging to the AP2/ERF, bHLH, bZIP and WRKY families were up or down deregulated (Fig. 7, conditions B and C). DEG in the CAMTA, FAR1, MYB-related, NAC and NF-Y families were predominantly down-regulated, while those in C2H2 and TCP families were upregulated. Interestingly, in plants challenged with both pests, the few deregulated TF genes concerned plants treated with aphids for 6 h, while only one DEG was found at 72 h of aphid treatment (Fig. 7, conditions F and G). This ~~suggesting~~ suggests a progressive loss of the deregulations of the TF transcripts triggered by aphids overtime. Similar analyses performed on DEG in the "hormone metabolism and signaling", "protein" categories clearly highlighted the disappearance of the aphid-induced deregulations in TuYV-infected plants (Suppl. Fig. 5 A and B).

Deregulation of the plant metabolome upon TuYV infection and aphid infestation

To investigate the downstream effects of the transcriptomic aphid-induced deregulations in the presence or absence of TuYV, we performed a targeted metabolomic profiling of the plants treated in conditions similar to those of the transcriptomic analysis (conditions A to G in Fig. 3A). We quantified in leaf samples the relative amounts of 59 identified metabolites involved in primary (18 amino acids, 8 organic acids and 4 sugars) and secondary metabolism (5 flavonoids, 14 glucosinolates, 5 hormones, 1 alkaloid and 4 isothiocyanates). These metabolites of interest were chosen based on their potential beneficial (amino acids, organic acids, sugars) or adverse (glucosinolates, flavonoids, alkaloids, isothiocyanates) effects towards aphids in the plant-aphid relationship.

Among the primary metabolites, some plant amino acids are essential nutrients for aphids. ~~Aphids cannot synthesize essential amino acids which are usually in short supply in phloem sap. Aphids therefore mostly rely on their symbionts to synthesize these amino acids (Hansen and Moran 2011). Sandström et al., (2000) showed that the aphid *Schizaphis graminum* increased the content of essential amino acids present in the phloem of host plants.~~ We therefore explored whether aphids, or ~~the aphid transmitted virus~~TuYV, could trigger the plant responses and alter some of the essential amino acids present in the plant. Globally, the virus alone had only a limited effect on the amino acids content in our conditions (Fig. 8, condition A). Aphids, on the other hand, displayed a more pronounced effect on the amino acid accumulation, especially on Isoleucine, Tyrosine and Serine, but also on Valine, Methionine, Lysine and Hydroxyproline (Fig. 8, condition B). This was particularly noticeable after 6 h of infestation while the changes tend to decline after 72 h of infestation. Interestingly, when both aggressors were present on the plant, the amino acid over-accumulation observed at 6 h post-infestation ~~were~~ was mostly maintained at 72 h post-infestation. Tyrosine and Proline were two amino acids that accumulated at high levels when aphids and TuYV were present (Fig. 8). Many significant increases could be assigned to aphids, as these effects were ~~sustained~~ maintained when the data were normalized with those of the virus (Fig. 8, conditions F and G). This contrasts with the results observed for the transcriptomic analysis where the deregulations induced by the aphid infestation on mock-inoculated plants were significantly lowered by the virus infection.

Sugar concentration has been reported to increase in aphid-infested Arabidopsis plants (Singh et al. 2011). We observed that in the condition of single virus infection or of single aphid infestation, there was a mild, but stable, over-accumulation of hexose and pentose (Fig. 8, conditions A, B and C). This increase was also observed in double treated plants (Fig. 8, conditions D and E). Raffinose and sucrose accumulated significantly and specifically in TuYV-infected plants regardless of the aphids (Fig. 8, conditions A, D and E). The sugar contents in double treated plants resembled those of TuYV-infected plants but with a massive increase in raffinose and a moderate increase in sucrose (Fig. 8, conditions D and E). When the data where normalized with virus-infected plant data, this effect was minored (case of raffinose), and

even abolished (for sucrose), which confirms that over-accumulation of these two sugars is mostly induced by virus infection alone regardless of the aphid presence (Fig. 8, conditions F and G).

Composition in organic acids was mainly modified in response to aphids in the presence of TuYV. Aphid infestation alone did not change significantly the accumulation of the eight compounds tested, except for the increase of malic acid and glucuronic acid at 6 h post-infestation (Fig. 8, conditions B and C). Viral infection alone had no effect on any of the organic acids tested (Fig. 8, condition A). On the other hand, plants with a dual treatment of aphids and virus showed an important increase of malic acid, gluconic acid, succinic acid, maleic acid, mucid acid and glucuronic acid content, with a major effect observed after 72 h of aphid infestation (Fig. 8, conditions D and E). Malic, maleic and mucid acids over-accumulations were already found after 6 h of aphid infestation (Fig. 8, condition D). This effect on the three organic acids was also observed, but with a lower intensity, when data were normalized with data from virus-infected plants (Fig. 8, condition G). This suggests that the deregulations ~~suggesting they~~ were partially triggered by aphids and partially by TuYV. An important decrease of citric acid accumulation was observed in TuYV-infected plants infested for 6 h (Fig. 8, condition D). Overall, these results suggest that several changes in sugar and organic acids leaf content are likely influenced by aphid infestation but more specifically in the presence of TuYV infection.

Plant synthesize a variety of secondary metabolites that can be detrimental to aphids (Nalam et al. 2019). Several studies have shown modifications in their accumulation upon aphid infestation (reviewed in (Louis et al. 2012b)). Complex hormonal changes triggered by aphids were also reported ((Eisenring et al. 2018); and reviews of (Morkunas et al. 2011), (Louis and Shah 2013) and (Züst and Agrawal 2016)). The results obtained here were contrasted, depending on the metabolite family. For flavonoids, camalexin or isothiocyanates no major change in accumulation was observed regardless of the different conditions (Fig. 8). Among the hormones analyzed, jasmonic acid and salicylic acid glucoside were found stable in all conditions. The jasmonic acid precursor oxo phytodienoic acid (OPDA), and to a lesser extent the auxin Indole-3-acetic-acid (IAA), over-accumulated specifically in doubled treated plants after 72 h of aphid infestation (Fig. 8, condition E). These modifications were also observed when data were normalized with

data from infected plants (Fig. 8, condition G), suggesting that there were induced by aphid infestation in infected plants but only at a late time of infestation. A similar effect in normalized data was found for salicylic acid at 72 h post-infestation only (Fig. 8, condition G), suggesting that the effect was induced by aphids in a viral context.

Glucosinolates (GSL) are a class of plant defensive compounds produced specifically in the *Brassicacae* family and conferring resistance against herbivores (Wittstock, Ute, Burow 2010). Their adverse effect on *M. persicae* is essentially due the consumption of the indole GLS present in phloem sap (Kim and Jander 2007). We found that among the 14 quantified GSL, only glucoesquerellin was reduced in plants after 72 h of aphid-infestation and in doubled treated plants (Fig. 8, conditions C and E). 1-hydroxy-glucobrassicin was the only GLS which accumulation increased massively in TuYV-infected plants (Fig. 8, condition A) and in doubled-treated plants (Fig. 8, conditions D and E). ~~but~~ This effect was however strongly alleviated when the data were normalized with data from virus-infected plants (Fig. 8, conditions F and G), suggesting that this change was essentially triggered by TuYV. The situation was more puzzling for 4-hydroxy-glucobrassicin, which accumulated only in infected plants after 72 h of aphid treatment. This effect was also observed at both time points when the data were normalized with those of TuYV-infected plants, pointing towards an aphid-deregulation specifically induced upon viral infection (Fig. 8, conditions F and G). Finally, a substantial over-accumulation of neoglucobracissin was found after 72 h post-treatment upon aphid and viral infection but only when the data were normalized with virus-infected plants data (Fig. 8, condition G). This effect could therefore be due to the aphids alone in TuYV-infected plants. Globally these results indicate that the level of a few specific indole GSL derived from the glucobrassicin compound increased in double aphid and viral-challenged plants mainly 72 h after aphid infestation. This increase in GLS triggered either by the virus or the aphid infestation could be responsible for specific effects on aphids in infected plants at a late stage of infestation.

Impact of aphid infestation on TuYV transmission

The aforementioned transcriptomic and metabolomics analyses revealed different patterns in the accumulation of mRNA and metabolites in plants infected with TuYV and infested with aphids for 6 h or 72 h compared to plants only infected with TuYV. To address the effect of such deregulations on transmission, we performed a series of TuYV transmission assays by *M. persicae* using as virus source *A. thaliana* Col-0 plants only infected with TuYV or infected and infested with aphids for 6 h or 72 h (corresponding to samples 1, 2 3 and 5, Fig. 2). The aphids used to pre-infest the plants for 6 h were manual removed and new non-viruliferous aphids were deposited on the infected plants for a 24 h acquisition period to analyze the capacity of these latter aphids to transmit the virus. After the 24 h acquisition period, the potentially viruliferous aphids were transferred to new Col-0 test plants for a 3-day inoculation period. Aphids were eliminated and the test plants were assayed by DAS-ELISA three weeks later. TuYV was transmitted to 68 to 95% of the test plants when aphids acquired TuYV on source plants that were not previously pre-infested (Table 1). We observed a statistically significant reduction of TuYV transmission by aphids when the source plants were previously infested by aphids for 6 h (42% and 57% of the test plants infected; Table 1, Exp.1 and 2), whereas no difference was observed when the virus source plants were previously infested for 72 h (53% to 68% of the test plants got infected; Table 1, Exp.3 to 5). The lower TuYV transmissibility from plants infected and infested with aphids for 6 h was not related to a lower virus titer in the virus source plants as TuYV accumulation measured by qRT-qPCR showed a similar virus titer in all source plants (plants only infected or infested with aphids for 6 h or 72 h) (Table 2). This indicates that an aphid pre-infestation of 72 h was beneficial to virus acquisition and transmission.

Discussion

This work addresses a genome wide andprovides a dynamic analysis of arabidopsis Arabidopsis plants attacked by two pestspathogens, the phloem-restricted virus TuYV and its aphid vector *M. persicae*, in order to decipher the genes specifically deregulated by the aphids in the presence or absence of the virus. Our transcriptomic data showed that TuYV infection relieved a majority of the gene deregulations

observed in aphid-infested *A. thaliana,* with a potential benefit to the aphid, and therefore, to the transmission of the virus. In accordance with our results, a particularly low level of gene deregulations was also observed by Chesnais et al. (2022) in Arabidopsis similarly infected with TuYV and infested with aphids. In our study~~,~~ the deregulation alleviations were significantly more important 72 h after aphid infestation than after 6 h. This ~~which~~ suggests that some delay is required after aphid infestation for the viral-infected plant to trigger the massive reduction of the plant responses switched on by the aphid infestation alone. The profile of the genes specifically deregulated by aphids that were unmodified in the presence of TuYV affected many gene categories (Fig. 6 and Suppl. Fig. 4) ~~among which~~ which include transcription factors, proteins and hormonal responses prone to induce substantial changes in host plant metabolism and physiology and interactions with aphids.

Deregulations of plant host transcription factors: a major virus-induced manipulation effect

~~The virus infection impact on the specifically aphid-induced plant response is particularly clear when we consider the transcriptomic profiles.~~ The major gene category which deregulation was greatly waived in TuYV-infected plants infested for 72 h was the transcription factors (TFs) category. Transcription factors specifically bind to promoters of target genes and act as transcriptional activators and repressors. There is increasing evidence that TFs genes play important roles in plant defense against phloem-feeding insects ((De Vos et al. 2005); (Gao et al. 2010); (Libault et al. 2007); (Rubil et al. 2022)). Among the genes that were deregulated in only aphid-infested plants, and not in infested and TuYV-infected plants, several TF-encoding gene families were over-represented like the AP2/ERF, FAR, MYB, NAC and WRKY families. These genes ~~which~~ are known to play crucial roles in abiotic and biotic stress responses. AP2/ERF encoding genes are key regulators of various abiotic stresses and are responsive to hormones like ethylene (ET) and abscisic acid (ABA) (Xie et al. 2019). Through their function in ET regulation, AP2/ERF factors influence the expression of defense-related genes (Abiri et al. 2017) and ET increase is known as a general defense response against herbivore~~s~~ attack (Bari and Jones 2009). AP2/ERF factors are also involved in the regulation of processes independent of ET signaling like the PHYTOALEXIN DEFICIENT 4 (PAD4) gene that

modulates the defense against *Myzus persicae* (Louis et al. 2012a). In our experiments, PAD4 gene expression was found induced among the genes deregulated by aphids and also by aphids and viral infection (conditions B, D and F respectively, Fig. 3). As we focused on aphid- or aphid and virus-specifically deregulated genes, genes like PAD4 were not retrieved after clustering aimed at identifying only the specifically deregulated genes (Fig. 5). Interestingly, some of the AP2/ERF factors were also found to be implicated in soybean responses to the aphid *Aphis glycines* (Yao et al. 2020).

The bHLH TF family is another family particularly deregulated in our aphid-infested plants that were not found in aphid-infested and TuYV-infected plants. Members of this gene family have already been reported to be affected in *A. thaliana* in response to another aphid species *Brevicorynae brassicae* (Barah et al. 2013). Another Several TF categories highlighted in Fig. 7y whose aphid-induced gene deregulation was alleviated by TuYV-infection is the bZIP family known to regulate ABA-responsive genes, are key regulators of biotic and abiotic stress responses (Lee and Luan 2012). For instance, the bZIP family is known to regulate ABA-responsive genes (Lee and Luan 2012), Among the C2H2 family is AtZAT6 of the C2H2 family which controls salicylic acid (SA) and reactive oxygen accumulation shown to be involved in multi-stress plant responses (Shi et al. 2014) and the. NAC TFs are are widely involved in different signaling pathways in response to different phytohormones and to abiotic or biotic stresses (Bian et al. 2021). Previous studies showed that NAC TFs could positively or negatively regulate plant defense responses but, at this point, it is hard to draw a general scheme of the mode of action of NAC TFs in our experimental set-up showing deregulation of these genes. However, considering their broad implication in hormone signaling (SA, JA, ABA, ET), any expression deregulation of these factors could have a subsequent effect on aphid behavior. Moreover, evidence of implication of these TFs in plant-virus interactions have been provided by several studies ((Yoshii et al. 2009); (Huang et al. 2017); (Selth et al. 2005)) suggesting that these deregulations could have a double impact on aphid infestation and virus infection.

MYB and WRKY TFs families are involved in plant defense responses to biotic stresses, in particular, following soybean response to aphids ((Yao et al. 2020); (Prochaska et al. 2015)), or aphid attack of *A. thaliana* ((Barah et al. 2013); (Louis and Shah 2013)). Several WRKY genes were found involved in plant

interactions with aphids inducing galls (Wang et al. 2017). A WRKY TF containing ankyrin domains was previously associated with wheat resistance to the aphid *Diuraphis noxia* (Nicolis and Venter 2018). Finally, FAR1 TFs play a crucial role in plant growth and development (Ma and Li 2018), and were reported to negatively modulate plant immunity and cell death., FAR1 TFs possibly ~~by interfering~~ interfere with ~~biosynthesis of~~ chlorophyll biosynthesis, ROS accumulation and SA signaling (Wang et al. 2016). FAR1 TFs were found deregulated in brown planthopper-induced or -constitutive resistance in rice, and represented the predominant family of TFs in the constitutive resistance to the insect (Wang et al. 2012). Interestingly, FAR1 genes were also involved in glucosinolate synthesis with a potential effect on plant-aphid interactions (Fernández-Calvo et al. 2020). Lastly, several auxin response factors (ARF) from the B3-superfamily of TFs were found to play a role in virus-plant interactions ((Zhao et al. 2022); (Müllender et al. 2021)).

Major gene deregulation in hormone biosynthesis and signaling, and protein degradation processes

Many of these TFs are directly or indirectly related to phytohormones which play a critical role in the regulation of plant-insect interactions. JA, SA and ET mediate plant defense against a wide range of herbivores including phloem-feeding insects like aphids ((Howe and Jander 2008); (Casteel et al. 2015); (Chapman et al. 2018); (Rubil et al. 2022)). In our study, genes directly involved in hormone synthesis and signaling pathways deregulated after aphid infestation, and reprogrammed by virus infection, were identified (Suppl. Fig. 5A). In particular, some gene deregulations in ABA, auxin, brassinosteroids, cytokinin, ET and JA pathways were specifically alleviated following TuYV infection suggesting that some of the plant-defense responses against aphids could be inhibited, with a potential benefit for virus acquisition by aphids. Mainly involved in regulating abiotic stress tolerance like drought responses, ABA has also been reported to play an important role in biotic stresses (Ton et al. 2009). Interestingly, in our experiments, all ABA-related genes were repressed in the presence of aphids at both time points while no deregulation was observed when the plants were additionally infected with TuYV (Suppl. Fig. 5A). Some viruses were reported to downregulate the ABA signaling pathway ((Westwood et al. 2013b); (Xie et al.

2018)). but Wwhether these modifications impact the aphid vector behavior, and therefore virus transmission, has not been addressed. Several genes involved in brassinosteroid biosynthesis and signaling pathways were found specifically deregulated by aphids only but not in presence of TuYV (Suppl. Fig. 5A). Theses hormones are known to play a role in response to pathogens (Nolan et al. 2020), but little is known in response to viral infection or to aphid infestation.

The JA pathway is one of the most efficient to inhibit herbivory (Howe and Jander 2008). Several plant viruses have been reported to manipulate the JA pathway to attract insect vectors ((Wu and Ye 2020); (Pan et al. 2021)). Some viral proteins responsible for these changes were identified. For instance, the 2b protein of cucumber mosaic virus (CMV) 2b protein directly interacts and inhibits the degradation of JAZ proteins which are transcriptional repressors of JA (Wu et al. 2017). The NS nonstructural protein of the tomato spotted wilt orthotospovirus and the ßC1 satellite of TYLCV bind MYC2 to impair JA activation pathway ((Li et al. 2014); (Wu et al. 2019)). Among the plant genes deregulated by only by aphids in our experiments, and which were common with previous studies, is *Jasmonate regulating gene 21* (also referred to as *JOX3*). It was down-regulated in both aphid infestation conditions (6 h and 72 h), but not in viral-infected plants. As JOX (Jasmonate-induced oxygenase) enzymes inactivate JA-Ile (Caarls et al. 2017), alleviation of *JOX3* repression could induce a potential beneficial effect on *M. persicae*. Following a targeted approach, (Patton et al. 2019) showed inhibition of expression of genes involved in phytohormone signaling pathways in plants aphid-infested and infected by the polerovirus potato leafroll virus (PLRV), when compared to plants only aphid-infested. Although the effect of these gene deregulations on PLRV transmission was not addressed, these results are perfectly in line with our large-scale analysis.

Another major category reprogrammed after virus infection is the “Protein” category with genes involved in protein synthesis and, responsible for post-translational modifications or protein degradation. There is increasing evidence that plant viruses affect protein degradation pathways to promote virus accumulation and attract their vectors by inhibiting plant defense responses. This is achieved mainly mediated by the

jasmonic acid defense pathway which inhibition is mediated by the TYLCV C2 protein (Li et al. 2019). In our study, subunits of several ubiquitin E3 ligases are among the most represented genes in the "Protein" category which deregulation upon aphids was relieved by TuYV infection. These proteins are part of the ubiquitin-proteasome system (UPS) and are classified into subfamilies based on their subunit responsible for the target recognition (~~ex HECT, RING...~~Miricescu et al., 2018). UPS has been reported to play an important role in plant defense response to biotic and abiotic stresses by regulating the biosynthesis and signaling of defense-related phytohormones or other related components ((Zhang et al. 2021); (Miricescu et al. 2018); (Kelley and Estelle 2012)). It is therefore conceivable that deregulations affecting protein degradation can subsequently affect vector behavior and virus uptake.

Interestingly, there is a tight interplay between hormonal and protein degradation pathways (Kelley and Estelle 2012) with potential consequences on vector behavior. Some viral proteins affect the JA pathway through a modification of the protein degradation pathway. For example, the P6 of the barley yellow striate mosaic rhabdovirus modified the SCF (Skp1/Cullin1/F-box) complex (Gao et al. 2022) with a subsequent effect on the JA-signaling pathway. Another example is the C2 protein of the monopartite begomovirus TYLCV, which interacts with plant ubiquitin 40S ribosomal protein S27a compromising JAZ degradation and the downstream expression of defense genes like the MYC2-regulated terpene synthase genes. This leads to alleviation of plant resistance to whitefly vectors (Li et al. 2019). A direct link between protein degradation and vector interaction was recently provided by Bera et al. (2022) who showed that turnip mosaic virus (TuMV) 6K1 protein could reprogram the plant protein degradation pathway. The viral protein reduced the abundance of JA biosynthesis-related transcripts and decreased plant protease activity in infected plants. In addition, TuMV infection downregulated expression of protease genes and upregulated expression of some autophagy and proteasome-related genes (Bera et al. 2022).

As ~~remarkably~~ highlighted by Ray and Casteel (Ray and Casteel 2022) in their review, viral and vector effectors have common host targets including transcription factors and protein turnover, suggesting that these interconnected pathways could play important functions in plant manipulation by vector-transmitted viruses.

Metabolomic profiles affected by aphid infestation and virus infection

Our preliminary ~~observations~~experiments designed to set up the time of aphid infestation in the dual transcriptomic and metabolomic analyses, ~~-~~showed that aphids triggered two main waves of metabolic changes, before and after 48 h post-infestation. These are in agreement with the results by (Tzin et al. 2015) who found a dynamic shift in the plant responses to aphid feeding, between the first hours of infestation by the aphid *Rhopalosiphum maidi*s and the later time points (after 48h) in maize. By choosing 6 and 72 ~~-~~h infestation, we ~~Such metabolic deregulations in non-infected *A. thaliana* plants are likely to be affected by additional biotic stresses, like the infection by an aphid-transmitted virus. Beside transcriptome deregulations, our experiments also addressed some plant metabolomic modifications triggered by aphid infestation and virus infection. We~~ observed distinct metabolic alterations in the presence of TuYV. P~~that~~ lants treated by both aphids and virus displayed changes that were significantly more important than those of aphid-treated plants. Moreover, the changes observed at 6 h post-infestation lasted up to 72 h. Conversely, ~~in~~ plants infested by aphids alone showed only faint alterations in metabolite accumulations ~~were only slightly modified~~ compared to mock-treated plants~~, while changes occurring in plants treated by both aphids and virus were significantly more important~~ and these tended to dissipate after 72 h (Fig. 8 compare conditions ~~B~~ D and ~~C~~ E with ~~D~~ B and ~~E~~C). ~~Interestingly, these changes occurred at 6 h post-infestation and lasted up to 72 h post-infestation, while in the case of plants only infested by aphids, the changes observed after 6 h tend to dissipate after 72 h.~~ Most of t~~T~~hese modifications could be ~~mostly~~ attributed to the aphids but only when plants were virus-infected ~~by virus~~. This was particularly visible for amino acids, organic acids and sugars.

As aphids cannot synthesize essential amino acids, which are usually in short supply in phloem sap, they~~.~~ ~~Aphids therefore mostly~~ rely on their symbionts to synthesize these amino acids (Hansen and Moran 2011). Sandström et al., (2000) showed that the aphid *Schizaphis graminum* increased the content of essential amino acids present in the phloem of host plants. The increase in a~~A~~mino acid~~s~~ and sugar~~s~~ content ~~increase~~ in ~~viral-infected and aphid-infected~~double-challenged plants~~, especially at later time,~~

could provide a positive effect on aphid growth and feeding behavior ((Mittler 1967)~~Mittler, 1967~~; (Ahmed et al. 2022)~~Ahmed et al., 2022~~) with a potential downstream effect on virus acquisition, especially at later time. Proline, a non-essential amino acid, was among the amino acids which accumulation raised specifically upon the double ~~pathogen~~ treatment, and particularly ~~strongly~~ at 72 h post-infestation. Proline is a multifunctional amino acid which level has been reported to increase in pathogen-related conditions, and could contribute to stress tolerance (Alvarez et al. 2022). Among the sugars analyzed, we observed a massive and specific increase in sucrose and raffinose in double treated plants at both times post aphid infestation, and not in single aphid infested plants. Sucrose is considered to be the sugar with the highest nutritional value for aphids. Moreover, sucrose is preferred to other sugars by aphids, including *M. persicae*, followed by raffinose (Hewer et al. 2010). As this effect was essentially induced by the virus, this indicates that TuYV ~~is able to~~can promote metabolic changes that favor aphid feeding, and therefore virus acquisition.

Surprisingly, some glucosinolates (GLS) which are expected to display a repellent effect, were also highly increased in plants treated with both ~~pathogens~~pests. This was the case for 1-OH glucobrassicin, 4-OH glucobrassicin and neoglucobrassicin, three indole GSL known to have an inhibitory effect on aphid proliferation ((Kim and Jander 2007); (Kim et al. 2008); (Pfalz et al. 2009)). Although GSL themselves are not toxic, their breakdown products generated by myrosinases, that are normally stored in separate cell types, act as defensive compounds against insect herbivores (Wittstock, Ute, Burow 2010). As aphids feed by causing minimal physical damage to cells surrounding the phloem, the negative effect of GSL on aphids is ~~limited but however real~~present but to a limited extent (Kim et al. 2008). Except 1-OH glucobrassicin which accumulation is induced by viral infection, accumulation of 4-OH glucobrassicin and neoglucobrassicin is specifically due to aphids in the presence of TuYV. Interestingly, these latter metabolites did accumulate massively at 72 h post-aphid infestation and could therefore constitute a signal for aphid dispersion under the control of the virus. Indeed, TuYV transmission follows a circulative mode and requires a latent period of several hours to circulate into the aphid's body and reach the accessory salivary glands before being inoculated (Brault et al. 2010). ~~It is therefore considered that~~

Ttthese toxic compounds over-accumulating at a late time of aphid infestation could therefore trigger aphid dispersion of the viruliferous aphids, as 72 h of aphid feeding is ~~widely~~ long enough for the aphids to acquire ~~a~~ sufficient ~~amount of~~ virus particles to transmit the virus.

~~Former~~ Previous studies showed that some indole GSL play an essential role in plant-virus-vector interactions. GSL synthesis is under the control of the MYC2 transcription factor which regulates the JA responsive genes (Dombrecht et al. 2007). ~~The interaction of the ßC1 protein expressed by the satellite of the whitefly transmitted begomovirus tomato yellow leaf curl China virus with MYC2 inhibits the~~ JA signaling and the downstream GSL synthesis ~~pathway~~ are both inhibited by the interaction of MYC2 with the ßC1 protein expressed by the whitefly-transmitted begomovirus tomato yellow leaf curl China virus (Li et al. 2014). This leads to the suppression of host resistance to whiteflies and further promotes begomovirus transmission. Another target of the ßC1 protein of a cotton begomovirus satellite is the transcription factor WRKY20 which regulates the synthesis of indole~~ic~~ GSL (Zhao et al. 2019). By interacting with WRKY20, ßC1 represses their synthesis which~~and thereby~~ benefits to the whitefly vector by increasing oviposition and the development of pupa. On the other hand, Arabidopsis plants infected with the Fny strain of CMV induced biosynthesis of the 4-methoxy glucobrassicin which inhibited phloem ingestion by aphids (Westwood et al. 2013a). ~~The~~ This GSL increase triggered by ~~authors demonstrated that~~ the viral RNA silencing suppressor 2b protein ~~is responsible for the upregulation of the 4-methoxy glucobrassicin, but this increase~~ is moderated by another viral protein, the 1a replicase, ensuring ~~thereby~~ that aphids were deterred from feeding but not poisoned. Altogether, this~~,~~ ~~promoting~~ could promote aphid dispersal and viral transmission. Since 4-methoxy glucobrassicin, which derives from 4-OH glucobrassicin, is considered as the most toxic indole GSL (Pfalz et al, 2009), the low over-accumulation of the former metabolite at a late time of aphid infestation in TuYV-infected plants could ~~participate to~~contribute to the dispersal of aphids ~~while~~ without ~~maintaining aphids alive~~causing mortality.

In contrast to the study reporting an induction of SA and JA in *Nicotiana benthamiana* and potato infested with *M. persicae* (Patton et al. 2019), we did not observe major modifications in the accumulation of both hormones in *A. thaliana* infested with this aphid species ~~in our study~~. However, Patton et al. (2019)

observed that these hormone deregulations (SA, JA and ET) were alleviated in *N. benthamiana* infected with PLRV. The hormonal modifications affected aphid settling and fecundity. Conversely, our results showed ~~a moderate~~only subtle ~~over-~~differences in SA and JA precursor accumulation~~, of SA and of the JA precursor~~ specifically at later time of aphid infestation in the presence of TuYV (Figure 8, conditions E and G). These opposite results ~~in the hormonal response~~ could be ~~either~~ due to ~~the pathosystem (potato-PLRV) or to~~ the experimental setting, as these hormone ~~accumulations~~ variations could be part of a transient response aimed to trigger aphid dispersal. Patton et al. (2019) showed that the hormonal response inhibition was under the control of the PLRV-encoded proteins P0 (the suppressor of RNA silencing), P1 (associated to replication) and P7 (a nucleic acid binding protein) (Delfosse et al. 2021).

Globally the ~~relief~~ reduction in~~of~~ gene deregulations observed in doubled treated plants points towards a complex interplay between phytohormonal pathways at different levels (transcription, protein degradation) to reduce or suppress the plant defenses against the vector, and subsequently to promote virus transmission.

It is noteworthy that the results found in our study did not lead to a conclusive correlation between metabolite accumulation and gene expression deregulation in similar samples. This may be explained by a time lag between transcription and the consequent changes at the metabolomic level, and the relatively moderate gene expression deregulations that were found among the specifically deregulated genes (Fig. 5). For instance, less than 10% of the genes specifically deregulated by aphids showed a $|\log_2 FC| \geq 1.5$ (9.8% and 9.0% respectively for 6 h and 72 h aphid infestation).

Despite predictions on pathogen transmission by vectors linked to the pathogen-induced deregulations (review in Mauck et al. (2019)), and theoretical models supporting that a plant infection inducing benefits to the vector, can have an impact on transmission ((Sisterson 2008); (Roosien et al. 2013); (Eigenbrode and Gomulkiewicz 2022); (Cunniffe et al. 2021)), no study has yet experimentally sustained these assertions. The effect of pathogen-induced plant gene deregulations on vector transmission can only be

addressed by conducting a temporal study of the effect of pathogen infection and/or vector development on the pathogen transmission efficiency. Such approach was developed in grapevine for the transmission of *Xylella fastidiosa* by its vector *Graphocephala atropunctata* (Zeilinger et al. 2021). At an early stage of bacterial infection, transmission was increased which coincided with an increase of the vector population size. At a later stage of infection, the transmission efficiency declined with increasing symptoms and plant avoidance of the vectors. Although we can suspect that early in bacterial infection plant defenses against the vector are reduced and would promote the vector population development, no molecular studies were conducted to sustain this hypothesis. In another pathosystem, phytoplasma infection was shown to reduce the grapevine defense response against the leafhopper vector, mostly mediated by the JA/ET pathways, but this transcriptional reprogramming was not correlated with transmission experiments (Bertazzon et al. 2019).

Conclusion

The major outcome of our study shows the highest efficiency of virus transmission when infected plants were pre-infested with aphids for 72 h, and this correlates with the alleviation of aphid-induced gene deregulations observed in plants similarly treated by aphids for 72 h. It provides to our knowledge the first experimental link between ~~a~~ viral-induced deregulation of plant-defense genes ~~against~~triggered by both ~~a~~the vector and the virus and virus- transmission by the vector.~~Conclusion~~ It therefore ~~Our study~~ reinforces the hypothesis that cross-talk regulations induced by different ~~aggressors~~ pests (in our case aphids and virus) can drive transcriptomic and metabolomic changes in plants with important consequences on virus-vector interactions, and a potential benefit for both ~~aggressors~~ pests when present simultaneously. ~~A major outbreak of our study is the correlation obtained between the widest alleviation of aphid-induced gene expression deregulation after 72 h infestation and the highest efficiency of virus transmission. The effect of pathogen-induced plant gene deregulations on vector transmission can only be addressed by conducting a temporal study of the effect of pathogen infection and/or vector development on the pathogen transmission efficiency.~~

This approach was developed in grapevine for the transmission of *Xylella fastidiosa* by its vector *Graphocephala atropunctata* (Zeilinger et al. 2021). At an early stage of bacterial infection, transmission was increased which coincided with an increase of the vector population size. At a later stage of infection, the transmission efficiency declined with increasing symptoms and plant avoidance of the vectors. Although we can suspect that early in bacterial infection plant defense against the vector are reduced and would induce the vector population development, no molecular studies were conducted to sustain this hypothesis. In another pathosystem, phytoplasma infection was shown to reduce the grapevine defense response against the leafhopper vector mostly mediated by the JA/ET pathways but this transcriptional reprogramming was not correlated with transmission experiments (Bertazzon et al. 2019). Despite predictions on pathogen transmission by vectors linked to the pathogen-induced deregulations (review in Mauck et al. (2019)), and theoretical models supporting that a plant infection inducing benefits to the vector can have an impact on the transmission ((Sisterson 2008); (Roosien et al. 2013); (Eigenbrode and Gomulkiewicz 2022); (Cunniffe et al. 2021)), our study provides to our knowledge the first experimental correlation between a pathogen-induced deregulation of plant-defense genes against vectors and the pathogen transmission by the vector.

Legends of figures

Figure 1: Time-dependent deregulations of differentially accumulated metabolites (red) in non-infected *A. thaliana* Col-0 upon aphid (*M. persicae*) infestation for 6, 24, 48, 72 and 96 h.

Figure 2: Experimental set-up for the high throughput metabolomic and transcriptomic analyses. Arabidopsis plants were inoculated with TuYV-viruliferous (upper panel) or non-viruliferous (lower panel) *M. persicae* aphids. After three weeks, the two batches of plants were infested with 30 non-viruliferous aphids for 6 or 72 h before harvesting (samples 3-4 and 5-6 respectively). Plants that were not infested with aphids were similarly processed (samples 1 and 2).

Figure 3: Comparison of the number of differentially expressed genes (DEG) obtained in the various conditions. **A.** Table illustrating the seven conditions analyzed in the next figures. The data of the five samples (Fig. 2 samples 1, 3, 4, 5 and 6) were normalized to data from mock-treated plants (sample 2) or to data from virus-infected plants (sample 1), to obtain the data of the seven experimental conditions A to G. These conditions will be resumed in the high throughput transcriptomic and metabolomic analyses. **B.** Number and representation of DEG found in the seven conditions. *Arabidopsis thaliana* plants (TuYV-infected or mock-inoculated) were treated with aphids for 0, 6 or 72 h. The total number of DEG are given for each condition below the graph, with the number of up and down-regulated genes below.

Figure 4: A. Comparison of gene expression between RNA-seq data and qRT-PCR. Samples of two biological repeats were used for qRT-PCR on a subset of twelve selected genes (in green and yellow). The data obtained were normalized using data from mock-inoculated plants and the results in the form of Log_2FC are presented for the conditions A to E (see Fig. 3A). **B.** Comparison of the Log-transformed gene expression ratios obtained from the RNA-seq data and qRT-PCR data for the twelve selected genes by a Pearson correlation test.

Figure 5: Hierarchical clustering analysis using the TIGR MultiExperiment Viewer (MeV). Six clusters were extracted from the DEG obtained in conditions B and C (plants only aphid-infested) and F and G (plants treated with aphids and TuYV). Cluster 1 corresponds to DEG from Arabidopsis plants infested with aphids at both 6 h and 72 h, cluster 2 at only 6 h infestation, cluster 3 at only 72 h infestation. Cluster 4, 5 and 6 contain genes specifically deregulated by aphids in TuYV-infected plants at both time points (cluster 4), at 6 h (cluster 5) and at 72 h (cluster 6) respectively. DEG that were found deregulated in any other conditions (e.g. at 6 h aphid infestation and 6 h aphid and TuYV treatment) were discarded. The number of DEG in each cluster is given in brackets next to the cluster number. The Log_2FC are given by shades of red and green colors according to the scale bar (red for down-regulated, green for up-regulated genes).

Figure 6: Differentially expressed genes (DEG) categorized into major Mapman bin code ontologies from *A. thaliana* infested by *M. persicae* only for 6 h or 72 h (conditions B and C, in yellow (6 h), red (72 h) and orange for the genes found at both time points, bars at the left from the separation bar) or in TuYV-

infected A. *thaliana* infested by *M. persicae* for 6 h or 72 h (conditions F and G, in light and dark green respectively and intermediate green for the genes found at both time points, bars at the right from the separation bar). The scale is the same for DEG at the right and left.

Figure 7: Representation of the mRNA deregulations affecting the transcription factors (TFs) genes by clustering them into different families and according to their down or up deregulation. The TFs were extracted from data corresponding to *A. thaliana* plants infested by *M. persicae* only for 6 h or 72 h (conditions B and C) and normalized to/with those of mock-treated plants or in TuYV-infected A. *thaliana* infested by *M. persicae* for 6 h or 72 h (conditions F and G) and normalized to those of viral-infected plants. The size of the circles is proportional to the number of deregulated TF genes (indicated in each circle).

Figure 8: Heatmap of significantly relative changes in metabolite patterns in *A. thaliana* plants treated by either TuYV (A), aphids alone for 6 h (condition B) or 72 h (condition C) or both pathogens for 6 h (conditions D and F) or 72 h (conditions E and G) aphid infestation. The data were normalized to mock-treated plants as indicated below the lanes (conditions A to E), or to viral-infected plants (conditions F and G). Metabolites were grouped accordingly to their functional or chemical family as amino acids, flavonoids, glucosinolates, hormones, alkaloids, organic acids, sugars and isothiocyanates, and their specific names is given at the right. Statistical analyses were performed using the Tukey's Honest Significant Difference method followed by a false discovery rate (FDR) correction, with FDR < 0.05. For FDR ≥ 0.05, Log_2FC were set to 0. The Log_2FC of significant metabolites for pairwise comparisons are given by shades of red or blue colors according to the scale bar at the right.

Supplemental data

Supplementary Table : Number of aligned reads for transcriptome profiling

Supplementary Table 2: List of primers used in real time PCR quantification (qRT-PCR) of selected genes or TuYV genome

Supplementary Table 3 : List of the 31 DEG common to plants infested by aphids for 5 or 6 h found in the data by Jaouannet et al. (2015) data, Bricchi et al. (2012) and our data.

Supplementary Figure S1: Venn diagram representing the overlap among DEG in the mock- and TuYV-infected plants after 6 and 72 h of aphid infestation. Green numbers indicate up-regulated DEG, red numbers indicate the down-regulated genes and the black numbers are the sum of up and down-regulated genes.

Supplementary Figure S2: Comparison of the transcriptomic data obtained in this study with data from the literature. **A.** Venn diagram illustrating the numbers of unique and common *A. thaliana* DEGs at early time of aphid infestation between Jaouannet et al. (2015) data (blue circle), Bricchi et al. (2012) (pink circle) data and our 6 h data (condition B, purple circle). Numbers in green represent up-regulated genes and those in red are down-regulated genes. Numbers at the left represent the common genes shared with our data. **B.** Venn diagram illustrating the numbers of unique and common *A. thaliana* DEGs after 72 h of aphid infestation between DeVos et al. (2005) results and ours (condition C). Below the bracket are the common genes.

Supplementary Figure S3: Gene ontology enrichment of biological processes performed on common genes identified between the data from Jaouannet et al. data (2015) (6 h), Bricchi et al. (2012) (5 h) and our early aphid infestation experiment (**A** and **B**) and those from DeVos et al. (2005) (72 h) and our late aphid infestation experiment (**C** and **D**). Down- (in red) and up-regulated (in green) genes were analyzed separately for each treatment. Gene ontology analysis was performed on David functional annotation tool (https://david.ncifcrf.gov/summary.jsp). p-values are indicated for each process.

Supplementary Figure S4: Gene ontology performed on differentially expressed genes (DEG) categorized into major Mapman bin code from **(A)** *A. thaliana* infested by *M. persicae* only (6 h and 72 h grouped together) (conditions B and C) or from **(B)** TuYV-infected A. *thaliana* infested by *M. persicae* for 6 h and 72 h (grouped together) (conditions F and G). Up-regulated genes are depicted in green and the down-regulated genes are in red.

~~**Supplementary Figure S5:** Clustering of mRNA deregulations of genes implicated in **(A)** hormonal responses and **(B)** genes fitting in the "protein" category. DEG were extracted from data corresponding to *A. thaliana* plants infested only by *M. persicae* for 6 h or 72 h (conditions B and C) and normalized to/with those of mock-treated plants or in TuYV infected A. *thaliana* infested by *M. persicae* for 6 h or 72 h (conditions F and G) and normalized to those of viral-infected plants. Up- and down-regulated genes are grouped. The size of the circles is proportional to the number of deregulated genes (indicated in each circle).~~

Acknowledgments. The authors would like to thank Claire Villeroy (INRAE Colmar) for the aphids rearing. Members of the experimental unit of INRAE, Colmar are acknowledged for the plant production. We are grateful to Malek Alioua and Sandrine Koechler for valuable assistance in ~~q~~RT-qPCR assays, Danièle Scheidecker for technical support and Magali Daujat for help in bioinformatic assistance.

References

Abiri, R., Shaharuddin, N. A., Maziah, M., Yusof, Z. N. B., Atabaki, N., Sahebi, M., et al. 2017. Role of ethylene and the APETALA 2/ethylene response factor superfamily in rice under various abiotic and biotic stress conditions. Environ. Exp. Bot. 134:33–44.

Ahmed, M. A., Ban, N., Hussain, S., Batool, R., Zhang, Y. J., Liu, T. X., et al. 2022. Preference and performance of the green peach aphid, Myzus persicae on three Brassicaceae vegetable plants and its association with amino acids and glucosinolates. PLoS One. 17:1–13 Available at: http://dx.doi.org/10.1371/journal.pone.0269736.

Alvarez, M. E., Savouré, A., and Szabados, L. 2022. Proline metabolism as regulatory hub. Trends Plant Sci. 27:39–55.

Anders, S., Pyl, P. T., and Huber, W. 2015. HTSeq-A Python framework to work with high-throughput sequencing data. Bioinformatics. 31:166–169.

878 Andrews, S. 2010. A quality control tool for high throughput sequence data.
879 https://www.bioinformatics.babraham.ac.uk/projects/fastqc/.
880 Bak, A., Cheung, A. L., Yang, C., Whitham, S. A., and Casteel, C. L. 2017. A viral protease relocalizes in
881 the presence of the vector to promote vector performance. Nat. Commun. 8:1–10.
882 Barah, P., Winge, P., Kusnierczyk, A., Tran, D. H., and Bones, A. M. 2013. Molecular Signatures in
883 Arabidopsis thaliana in Response to Insect Attack and Bacterial Infection. PLoS One. 8.
884 Bari, R., and Jones, J. D. G. 2009. Role of plant hormones in plant defence responses. Plant Mol. Biol.
885 69:473–488.
886 Bera, S., Arena, G. D., Ray, S., Flannigan, S., and Casteel, C. L. 2022. The Potyviral Protein 6K1 Reduces
887 Plant Proteases Activity during Turnip mosaic virus Infection. Viruses. 14:1–16.
888 Bera, S., Blundell, R., Liang, D., Crowder, D. W., and Casteel, C. L. 2020. The Oxylipin Signaling
889 Pathway Is Required for Increased Aphid Attraction and Retention on Virus-Infected Plants. J. Chem.
890 Ecol. 46:771–781.
891 Bertazzon, N., Bagnaresi, P., Forte, V., Mazzucotelli, E., Filippin, L., Guerra, D., et al. 2019. Grapevine
892 comparative early transcriptomic profiling suggests that Flavescence dorée phytoplasma represses
893 plant responses induced by vector feeding in susceptible varieties. BMC Genomics. 20:1–27.
894 Berthelot, E., Ducousso, M., Macia, J.-L., Bogaert, F., Baecker, V., Thébaud, G., et al. 2019. Turnip
895 Mosaic Virus Is a Second Example of a Virus Using Transmission Activation for Plant-to-Plant
896 Propagation by Aphids. J. Virol. 93:1–11.
897 Bian, Z., Gao, H., and Wang, C. 2021. NAC transcription factors as positive or negative regulators
898 during ongoing battle between pathogens and our food crops. Int. J. Mol. Sci. 22:1–21.
899 Bragard, C., Caciagli, P., Lemaire, O., Lopez-Moya, J. J., Macfarlane, S., Peters, D., et al. 2013. Status
900 and prospects of plant virus control through interference with vector transmission. Annu. Rev.
901 Phytopathol. 51:177–201.
902 Brault, V., Uzest, M., Monsion, B., Jacquot, E., and Blanc, S. 2010. Aphids as transport devices for
903 plant viruses. Comptes Rendus - Biol. 333:524–538.

Bricchi, I., Bertea, C. M., Occhipinti, A., Paponov, I. A., and Maffei, M. E. 2012. Dynamics of Membrane Potential Variation and Gene Expression Induced by Spodoptera littoralis, Myzus persicae, and Pseudomonas syringae in Arabidopsis. PLoS One. 7.

Bruyère, A., Brault, V., Ziegler-Graff, V., Simonis, M.-T. T., Van Den Heuvel, J. F. J. M. F. J. M., Richards, K., et al. 1997. Effects of mutations in the beet western yellows virus readthrough protein on its expression and packaging and on virus accumulation, symptoms, and aphid transmission. Virology. 230:323–334.

Caarls, L., Elberse, J., Awwanah, M., Ludwig, N. R., De Vries, M., Zeilmaker, T., et al. 2017. Arabidopsis JASMONATE-INDUCED OXYGENASES down-regulate plant immunity by hydroxylation and inactivation of the hormone jasmonic acid. Proc. Natl. Acad. Sci. U. S. A. 114:6388–6393.

Carr, J. P., Donnelly, R., Tungadi, T., Murphy, A. M., Jiang, S., Bravo-Cazar, A., et al. 2018. Viral Manipulation of Plant Stress Responses and Host Interactions With Insects. Adv. Virus Res. 102:177–197.

Carr, J. P., Tungadi, T., Donnelly, R., Bravo-Cazar, A., Rhee, S. J., Watt, L. G., et al. 2020. Modelling and manipulation of aphid-mediated spread of non-persistently transmitted viruses. Virus Res. 277.

Casteel, C. L., De Alwis, M., Bak, A., Dong, H., Whitham, S. A., and Jander, G. 2015. Disruption of Ethylene Responses by *Turnip mosaic virus* Mediates Suppression of Plant Defense against the Green Peach Aphid Vector. Plant Physiol. 169:209–218 Available at: http://www.plantphysiol.org/lookup/doi/10.1104/pp.15.00332.

Chapman, K. M., Marchi-Werle, L., Hunt, T. E., Heng-Moss, T. M., and Louis, J. 2018. Abscisic and Jasmonic Acids Contribute to Soybean Tolerance to the Soybean Aphid (Aphis glycines Matsumura). Sci. Rep. 8:1–12 Available at: http://dx.doi.org/10.1038/s41598-018-33477-w.

Chesnais, Q., Golyaev, V., Velt, A., Rustenholz, C., Brault, V., Pooggin, M. M., et al. 2022. Comparative Plant Transcriptome Profiling of Arabidopsis thaliana Col-0 and Camelina sativa var. Celine Infested with Myzus persicae Aphids Acquiring Circulative and Noncirculative Viruses Reveals Virus- and Plant-Specific Alterations Relevant to Aphid F. Microbiol. Spectr. 10.

930 Clark, M. F., and Adams, A. N. 1977. Characteristics of the microplate method of enzyme linked
931 immunosorbent assay for the detection of plant viruses. J. Gen. Virol. 34:475–483.
932 Cunniffe, N. J., Taylor, N. P., Hamelin, F. M., and Jeger, M. J. 2021. *Epidemiological and ecological*
933 *consequences of virus manipulation of host and vector in plant virus transmission*.
934 Dáder, B., Then, C., Berthelot, E., Ducousso, M., Ng, J. C. K., and Drucker, M. 2017. Insect
935 transmission of plant viruses: Multilayered interactions optimize viral propagation. Insect Sci.
936 24:929–946.
937 Delfosse, V. C., Barrios Barón, M. P., and Distéfano, A. J. 2021. What we know about poleroviruses:
938 Advances in understanding the functions of polerovirus proteins. Plant Pathol. 70:1047–1061.
939 Dietzgen, R. G., Mann, K. S., and Johnson, K. N. 2016. Plant virus-insect vector interactions: Current
940 and potential future research directions. Viruses. 8:1–21.
941 Dombrecht, B., Gang, P. X., Sprague, S. J., Kirkegaard, J. A., Ross, J. J., Reid, J. B., et al. 2007. MYC2
942 differentially modulates diverse jasmonate-dependent functions in Arabidopsis. Plant Cell. 19:2225–
943 2245.
944 Eigenbrode, S. D., Bosque-Pérez, N. A., and Davis, T. S. 2018. Insect-Borne Plant Pathogens and Their
945 Vectors: Ecology, Evolution, and Complex Interactions. Annu. Rev. Entomol. 63:169–191.
946 Eigenbrode, S. D., and Gomulkiewicz, R. 2022. Manipulation of Vector Host Preference by Pathogens:
947 Implications for Virus Spread and Disease Management. J. Econ. Entomol. 115:387–400.
948 Eisenring, M., Glauser, G., Meissle, M., and Romeis, J. 2018. Differential Impact of Herbivores from
949 Three Feeding Guilds on Systemic Secondary Metabolite Induction, Phytohormone Levels and Plant-
950 Mediated Herbivore Interactions. J. Chem. Ecol. 44:1178–1189.
951 Fernández-Calvo, P., Iñigo, S., Glauser, G., Vanden Bossche, R., Tang, M., Li, B., et al. 2020. FRS7 and
952 FRS12 recruit NINJA to regulate expression of glucosinolate biosynthesis genes. New Phytol.
953 227:1124–1137.
954 Gao, D.-M., Zhang, Z.-J., Qiao, J.-H., Gao, Q., Zang, Y., Xu, W.-Y., et al. 2022. A rhabdovirus accessory
955 protein inhibits jasmonic acid signaling in plants to attract insect vectors. Plant Physiol. 190:1349–

1364.

Gao, L. L., Kamphuis, L. G., Kakar, K., Edwards, O. R., Udvardi, M. K., and Singh, K. B. 2010. Identification of potential early regulators of aphid resistance in Medicago truncatula via transcription factor expression profiling. New Phytol. 186:980–994.

Hansen, A. K., and Moran, N. A. 2011. Aphid genome expression reveals host-symbiont cooperation in the production of amino acids. Proc. Natl. Acad. Sci. U. S. A. 108:2849–2854.

Hewer, A., Will, T., and Van Bel, A. J. E. 2010. Plant cues for aphid navigation in vascular tissues. J. Exp. Biol. 213:4030–4042.

Howe, E., Holton, K., Nair, S., Schlauch, D., Sinha, R., and Quackenbush, J. 2010. MeV: MultiExperiment Viewer. Biomed. Informatics Cancer Res. :267–277.

Howe, G. A., and Jander, G. 2008. Plant Immunity to Insect Herbivores. Annu. Rev. Plant Biol. 59:41–66.

Hu, J., Huang, J., Xu, H., Wang, Y., Li, C., Wen, P., et al. 2020. Rice stripe virus suppresses jasmonic acid-mediated resistance by hijacking brassinosteroid signaling pathway in rice. PLoS Pathog. 16:1–23 Available at: http://dx.doi.org/10.1371/journal.ppat.1008801.

Huang, D. W., Sherman, B. T., Tan, Q., Collins, J. R., Alvord, W. G., Roayaei, J., et al. 2007. The DAVID Gene Functional Classification Tool: A novel biological module-centric algorithm to functionally analyze large gene lists. Genome Biol. 8.

Huang, Y., Li, T., Xu, Z. S., Wang, F., and Xiong, A. S. 2017. Six NAC transcription factors involved in response to TYLCV infection in resistant and susceptible tomato cultivars. Plant Physiol. Biochem. 120:61–74 Available at: https://doi.org/10.1016/j.plaphy.2017.09.020.

J. M. van den Heuvel, J. F. 1991. Transmission of Potato Leafroll Virus from Plants and Artificial Diets by Myzus persicae . Phytopathology. 81:150.

Jaouannet, M., Morris, J. A., Hedley, P. E., and Bos, J. I. B. 2015. Characterization of Arabidopsis Transcriptional Responses to Different Aphid Species Reveals Genes that Contribute to Host Susceptibility and Non-host Resistance. :1–26 Available at:

http://dx.doi.org/10.1371/journal.ppat.1004918.

Jayasinghe, W. H., Kim, H., Nakada, Y., and Masuta, C. 2021. A plant virus satellite RNA directly accelerates wing formation in its insect vector for spread. Nat. Commun. 12:1–10.

Kelley, D. R., and Estelle, M. 2012. Ubiquitin-mediated control of plant hormone signaling. Plant Physiol. 160:47–55.

Kim, D., Langmead, B., and Salzberg, S. L. 2015. HISAT: A fast spliced aligner with low memory requirements. Nat. Methods. 12:357–360.

Kim, J. H., and Jander, G. 2007. Myzus persicae (green peach aphid) feeding on Arabidopsis induces the formation of a deterrent indole glucosinolate. Plant J. 49:1008–1019.

Kim, J. H., Lee, B. W., Schroeder, F. C., and Jander, G. 2008. Identification of indole glucosinolate breakdown products with antifeedant effects on Myzus persicae (green peach aphid). Plant J. 54:1015–1026.

Lee, S. C., and Luan, S. 2012. ABA signal transduction at the crossroad of biotic and abiotic stress responses. Plant, Cell Environ. 35:53–60.

Li, P., Liu, C., Deng, W. H., Yao, D. M., Pan, L. L., Li, Y. Q., et al. 2019. Plant begomoviruses subvert ubiquitination to suppress plant defenses against insect vectors. PLoS Pathog. 15.

Li, R., Weldegergis, B. T., Li, J., Jung, C., Qu, J., Sun, Y., et al. 2014. Virulence factors of geminivirus interact with MYC2 to subvert plant resistance and promote vector performance. Plant Cell. 26:4991–5008 Available at: https://www.ncbi.nlm.nih.gov/pubmed/25490915.

Libault, M., Wan, J., Czechowski, T., Udvardi, M., and Stacey, G. 2007. Identification of 118 Arabidopsis transcription factor and 30 ubiquitin-ligase genes responding to chitin, a plant-defense elicitor. Mol. Plant-Microbe Interact. 20:900–911.

Louis, J., Mondal, H. A., and Shah, J. 2012a. Green peach aphid infestation induces Arabidopsis PHYTOALEXIN-DEFICIENT4 expression at site of insect feeding. Plant Signal. Behav. 7:1431–1433.

Louis, J., and Shah, J. 2013. Arabidopsis thaliana — Myzus persicae interaction : shaping the understanding of plant defense against phloem-feeding aphids. Front. Plant Sci. 4:1–18.

Louis, J., Singh, V., and Shah, J. 2012b. Arabidopsis thaliana —Aphid Interaction. Arab. B. 10:e0159.

Love, M. I., Huber, W., and Anders, S. 2014. Moderated estimation of fold change and dispersion for RNA-seq data with DESeq2. Genome Biol. 15:1–21.

Ma, L., and Li, G. 2018. FAR1-RELATED SEQUENCE (FRS) AND FRS-RELATED FACTOR (FRF) family proteins in arabidopsis growth and development. Front. Plant Sci. 9:1–10.

Marmonier, A., Velt, A., Villeroy, C., Rustenholz, C., Chesnais, Q., and Brault, V. 2022. Differential gene expression in aphids following virus acquisition from plants or from an artificial medium. BMC Genomics. 23:1–15 Available at: https://doi.org/10.1186/s12864-022-08545-1.

Martinière, A., Bak, A., Macia, J. L., Lautredou, N., Gargani, D., Doumayrou, J., et al. 2013. A virus responds instantly to the presence of the vector on the host and forms transmission morphs. Elife. 2013:1–26.

Mauck, K., Bosque-Pérez, N. A., Eigenbrode, S. D., De Moraes, C. M., and Mescher, M. C. 2012. Transmission mechanisms shape pathogen effects on host-vector interactions: Evidence from plant viruses. Funct. Ecol. 26:1162–1175.

Mauck, K. E. 2016. Variation in virus effects on host plant phenotypes and insect vector behavior: what can it teach us about virus evolution? Curr. Opin. Virol. 21:114–123.

Mauck, K. E., Chesnais, Q., and Shapiro, L. R. 2018. *Evolutionary Determinants of Host and Vector Manipulation by Plant Viruses*. 1st ed. Elsevier Inc. Available at: http://dx.doi.org/10.1016/bs.aivir.2018.02.007.

Mauck, K. E., Kenney, J., and Chesnais, Q. 2019. Progress and challenges in identifying molecular mechanisms underlying host and vector manipulation by plant viruses. Curr. Opin. Insect Sci. :7–18.

Miricescu, A., Goslin, K., and Graciet, E. 2018. Ubiquitylation in plants: Signaling hub for the integration of environmental signals. J. Exp. Bot. 69:4511–4527.

Mishra, M., Mahajan, N., Tamhane, V. A., Kulkarni, M. J., Baldwin, I. T., Gupta, V. S., et al. 2012. Stress inducible proteinase inhibitor diversity in Capsicum annuum. BMC Plant Biol. 12.

Mittler, T. E. 1967. Effect on aphid feeding of dietary methionine [17]. Nature. 214:386.

Morkunas, I., Mai, V. C., and Gabryś, B. 2011. Phytohormonal signaling in plant responses to aphid feeding. Acta Physiol. Plant. 33:2057–2073.

Müllender, M., Varrelmann, M., Savenkov, E. I., and Liebe, S. 2021. Manipulation of auxin signalling by plant viruses. Mol. Plant Pathol. 22:1449–1458.

Nalam, V., Louis, J., and Shah, J. 2019. Plant defense against aphids, the pest extraordinaire. Plant Sci. 279:96–107.

Nicolis, V., and Venter, E. 2018. Silencing of a unique integrated domain nucleotide-binding leucine-rich repeat gene in wheat abolishes diuraphis noxia resistance. Mol. Plant-Microbe Interact. 31:940–950.

Nolan, T. M., Vukasinović, N., Liu, D., Russinova, E., and Yin, Y. 2020. Brassinosteroids: Multidimensional regulators of plant growth, development, and stress responses. Plant Cell. 32:298–318.

Pan, L. L., Miao, H., Wang, Q., Walling, L. L., and Liu, S. S. 2021. Virus-induced phytohormone dynamics and their effects on plant–insect interactions. New Phytol. 230:1305–1320.

Patton, M. K. F., Bak, A., M., S. J., and Heck, M. L. 2019. A polerovirus, Potatao leafroll virus, alters plant-vector ineractions using three viral proteins. Plant Cell Env. :1–13.

Pfalz, M., Vogel, H., and Kroymann, J. 2009. The gene controlling the Indole Glucosinolate Modifier1 quantitative trait locus alters indole glucosinolate structures and aphid resistance in Arabidopsis. Plant Cell. 21:985–999.

Prochaska, T. J., Donze-Reiner, T., Marchi-Werle, L., Palmer, N. A., Hunt, T. E., Sarath, G., et al. 2015. Transcriptional responses of tolerant and susceptible soybeans to soybean aphid (Aphis glycines Matsumura) herbivory. Arthropod. Plant. Interact. 9:347–359.

Ray, S., and Casteel, C. L. 2022. Effector-mediated plant – virus – vector interactions. Plant Cell. :1–18.

Ritchie, M. E., Phipson, B., Wu, D., Hu, Y., Law, C. W., Shi, W., et al. 2015. Limma powers differential expression analyses for RNA-sequencing and microarray studies. Nucleic Acids Res. 43:e47.

Roosien, B. K., Gomulkiewicz, R., Ingwell, L. L., Bosque-Pérez, N. A., Rajabaskar, D., and Eigenbrode, S. D. 2013. Conditional Vector Preference Aids the Spread of Plant Pathogens: Results From a Model. Environ. Entomol. 42:1299–1308.

Rubil, N., Kalachova, T., Hauser, T. P., and Burketová, L. 2022. Specialist Aphid Feeding Causes Local Activation of Salicylic and Jasmonic Acid Signaling in Arabidopsis Veins. Mol. Plant-Microbe Interact. 35:119–124.

Sandström, J., Telang, A., and Moran, N. A. 2000. Nutritional enhancement of host plants by aphids — a comparison of three aphid species on grasses. J. Insect Physiol. 46:33–40.

Selth, L. A., Dogra, S. C., Rasheed, M. S., Healy, H., Randles, J. W., and Rezaian, M. A. 2005. A NAC domain protein interacts with Tomato leaf curl virus replication accessory protein and enhances viral replication. Plant Cell. 17:311–325.

Shi, H., Wang, X., Ye, T., Chen, F., Deng, J., Yang, P., et al. 2014. The cysteine2/histidine2-type transcription factor zinc finger of arabidopsis thaliana6 modulates biotic and abiotic stress responses by activating salicylic acid-related genes and c-repeat-binding factor genes in arabidopsis. Plant Physiol. 165:1367–1379.

Singh, V., Louis, J., Ayre, B. G., Reese, J. C., and Shah, J. 2011. TREHALOSE PHOSPHATE SYNTHASE11-dependent trehalose metabolism promotes Arabidopsis thaliana defense against the phloem-feeding insect Myzus persicae. Plant J. 67:94–104.

Sisterson, M. S. 2008. Effects of insect-vector preference for healthy or infected plants on pathogen spread: Insights from a model. J. Econ. Entomol. 101:1–8.

Thimm, O., Bläsing, O., Gibon, Y., Nagel, A., Meyer, S., Krüger, P., et al. 2004. MAPMAN: A user-driven tool to display genomics data sets onto diagrams of metabolic pathways and other biological processes. Plant J. 37:914–939.

Ton, J., Flors, V., and Mauch-Mani, B. 2009. The multifaceted role of ABA in disease.pdf. Trends Plant Sci. :310–317 Available at: http://www.sciencedirect.com/science/article/pii/S1360138509001198.

Tzin, V., Fernandez-Pozo, N., Richter, A., Schmelz, E. A., Schoettner, M., Schäfer, M., et al. 2015.

1086 Dynamic maize responses to aphid feeding are revealed by a time series of transcriptomic and
1087 metabolomic assays. Plant Physiol. 169:1727–1743.
1088 De Vos, M., Van Oosten, V. R., Van Poecke, R. M., Van Pelt, J. A., Pozo, M. J., Mueller, M. J., et al.
1089 2005. Signal signature and transcriptome changes of Arabidopsis during pathogen and insect attack.
1090 Mol Plant Microbe Interact. 18:923–937 Available at:
1091 http://www.ncbi.nlm.nih.gov/entrez/query.fcgi?cmd=Retrieve&db=PubMed&dopt=Citation&list_uid
1092 s=16167763.
1093 Wamonje, F. O., Donnelly, R., Tungadi, T. D., Murphy, A. M., Pate, A. E., Woodcock, C., et al. 2020.
1094 Different Plant Viruses Induce Changes in Feeding Behavior of Specialist and Generalist Aphids on
1095 Common Bean That Are Likely to Enhance Virus Transmission. Front. Plant Sci. 10:1–13.
1096 Wang, H., Cui, K., Shao, S., Liu, J., Chen, H., Wang, C., et al. 2017. Molecular response of gall induction
1097 by aphid schlechtendalia chinensis (Bell) attack on Rhus chinensis mill. J. Plant Interact. 12:465–479.
1098 Wang, W., Tang, W., Ma, T., Niu, D., Jin, J. B., Wang, H., et al. 2016. A pair of light signaling factors
1099 FHY3 and FAR1 regulates plant immunity by modulating chlorophyll biosynthesis. J. Integr. Plant Biol.
1100 58:91–103.
1101 Wang, Y., Guo, H., Li, H., Zhang, H., and Miao, X. 2012. Identification of transcription factors potential
1102 related to brown planthopper resistance in rice via microarray expression profiling. BMC Genomics.
1103 13.
1104 Westwood, J. H., Groen, S. C., Du, Z., Murphy, A. M., Anggoro, D. T., Tungadi, T., et al. 2013a. A trio of
1105 viral proteins tunes aphid-plant interactions in arabidopsis thaliana. PLoS One. 8:1–18.
1106 Westwood, J. H., Mccann, L., Naish, M., Dixon, H., Murphy, A. M., Stancombe, M. A., et al. 2013b. A
1107 viral RNA silencing suppressor interferes with abscisic acid-mediated signalling and induces drought
1108 tolerance in Arabidopsis thaliana. Mol. Plant Pathol. 14:158–170.
1109 Whitfield, A. E., Falk, B. W., and Rotenberg, D. 2015. Insect vector-mediated transmission of plant
1110 viruses. Virology. 479–480:278–289.
1111 Wittstock, Ute, Burow, M. 2010. Glucosinolate Breakdown in Arabidopsis : Mechanism , Regulation

and Biological Significance. Arab. B.

Wu, D., Qi, T., Li, W. X., Tian, H., Gao, H., Wang, J., et al. 2017. Viral effector protein manipulates host hormone signaling to attract insect vectors. Cell Res. 27:402–415 Available at: https://www.ncbi.nlm.nih.gov/pubmed/28059067.

Wu, X., Xu, S., Zhao, P., Zhang, X., Yao, X., Sun, Y., et al. 2019. The orthotospovirus nonstructural protein NSs suppresses plant MYC-regulated jasmonate signaling leading to enhanced vector attraction and performance. PLoS Pathog. 15:1–21.

Wu, X., and Ye, J. 2020. Manipulation of jasmonate signaling by plant viruses and their insect vectors. Viruses. 12.

Xie, K., Li, L., Zhang, H., Wang, R., Tan, X., He, Y., et al. 2018. Abscisic acid negatively modulates plant defence against rice black-streaked dwarf virus infection by suppressing the jasmonate pathway and regulating reactive oxygen species levels in rice. Plant Cell Environ. 41:2504–2514 Available at: https://onlinelibrary.wiley.com/doi/10.1111/pce.13372.

Xie, Z., Nolan, T. M., Jiang, H., and Yin, Y. 2019. AP2/ERF transcription factor regulatory networks in hormone and abiotic stress responses in Arabidopsis. Front. Plant Sci. 10:1–17.

Xu, H., Luo, X., Qian, J., Pang, X., Song, J., Qian, G., et al. 2012. FastUniq: A Fast De Novo Duplicates Removal Tool for Paired Short Reads. PLoS One. 7:1–6.

Yao, L., Yang, B., Ma, X., Wang, S., Guan, Z., Wang, B., et al. 2020. A genome-wide view of transcriptional responses during aphis glycines infestation in soybean. Int. J. Mol. Sci. 21:1–19.

Yoshii, M., Shimizu, T., Yamazaki, M., Higashi, T., Miyao, A., Hirochika, H., et al. 2009. Disruption of a novel gene for a NAC-domain protein in rice confers resistance to Rice dwarf virus. Plant J. 57:615–625.

Zeilinger, A. R., Wallis, C. M., Beal, D., Sicard, A., Walker, M. A., and Almeida, R. P. P. 2021. Plant defense against a pathogen drives nonlinear transmission dynamics through both vector preference and acquisition. Ecosphere. 12.

Zhang, Y., Chen, M., Zhou, S., Lou, Y., and Lu, J. 2021. Silencing an E3 ubiquitin ligase gene OsJMJ715

enhances the resistance of rice to a piercing-sucking herbivore by activating ABA and JA signaling pathways. Int. J. Mol. Sci. 22.

Zhao, L., Zhang, L., Hu, Z., Li, B., Zheng, X., Qiu, R., et al. 2022. Tomato zonate spot virus induced hypersensitive resistance via an auxin-related pathway in pepper. Gene. 823:146320.

Zhao, P., Yao, X., Cai, C., Li, R., Du, J., Sun, Y., et al. 2019. Viruses mobilize plant immunity to deter nonvector insect herbivores. Sci. Adv. 5:eaav9801.

Ziegler-Graff, V. 2020. Molecular insights into host and vector manipulation by plant viruses. Viruses. 12.

Züst, T., and Agrawal, A. A. 2016. Mechanisms and evolution of plant resistance to aphids. Nat. Plants. 2:1–9 Available at: http://dx.doi.org/10.1038/nplants.2015.206.

TABLE 1. TuYV aphid transmission assays from TuYV-infected and infested plants

	Nb plants infected/ inoculated[a]				
Source plants	**Exp. 1**	**Exp. 2**	**Exp. 3**	**Exp. 4**	**Exp. 5**
TuYV	41/60 (68%)	57/60 (95%)	45/60 (75%)	43/60 (72%)	48/60 (80%)
TuYV + 6h aphid infestation	25/60 (42%)	34/60 (57%)	/	/	/
TuYV + 72h aphid infestation	/	/	37/60 (62%)	32/60 (53%)	41/60 (68%)
pvalue[b]	***0.005***	***9.13e-7***	*0.17*	*0.17*	*0.21*

[a]Number of plants infected/total number of plants inoculated and assayed by DAS-ELISA. Percentage of infected plants in brackets. A plant is considered infected when the optical density (OD) value of the leaf extract is above twice the mean OD values of three non-infected plants plus three times the standard deviation of these values.

[b] Mann-Whitney U test

TABLE 2. TuYV genome accumulation measured by RT-qPCR in source plants

	Nb TuYV genomes/µg RNA ± SD[a]	
Source plants	**Exp. 1**	**Exp. 2**
TuYV	9.08E+05 ± 1.71E+05	7.90E+05 ± 1.01E+05
TuYV + 6 h aphid infestation	6.73E+05 ± 3.44E+05	/
TuYV + 7 2h aphid infestation	/	9.27E+05 ± 3.38E+05
p-value[b]	*0.530*	*0.918*

[a]Mean value of TuYV genomes in three samples/total RNA ± Standard deviation (SD)

[b]Paired t-test

Legends of figures

Figure 1: Time-dependent deregulations of differentially accumulated metabolites (red) in non-infected *A. thaliana* Col-0 upon aphid (*M. persicae*) infestation for 6, 24, 48, 72 and 96 h.

Figure 2: Experimental set-up for the high throughput transcriptomic and metabolomic analyses. Arabidopsis plants were inoculated with TuYV-viruliferous (upper panel) or non-viruliferous (lower panel) *M. persicae* aphids. After three weeks, the two batches of plants were infested with 30 non-viruliferous aphids for 6 or 72 h before harvesting (samples 3-4 and 5-6 respectively). Plants that were not infested with aphids were similarly processed (samples 1 and 2).

Figure 3: Comparison of the number of differentially expressed genes (DEG) obtained in the various conditions. **A.** Table illustrating the seven conditions analyzed in the next figures. The data of the five samples (Fig. 2 samples 1, 3, 4, 5 and 6) were normalized to data from mock-treated plants (sample 2) or to data from virus-infected plants (sample 1), to obtain the data of the seven experimental conditions A to G. These conditions will be resumed in the high throughput transcriptomic and metabolomic analyses. **B.** Number and representation of DEG found in the seven conditions. *Arabidopsis thaliana* plants (TuYV-infected or mock-inoculated) were infested with aphids for 0, 6 or 72 h. The total number of DEG are given for each condition below the graph, with the number of up and down-regulated genes below.

Figure 4: A. Comparison of gene expression between RNA-seq data and RT-qPCR analysis. Samples of two biological repeats were used for RT-qPCR on a subset of twelve selected genes (in green and yellow). The data obtained were normalized using data from mock-inoculated plants and the results in the form of log_2FC are presented for the conditions A to E (see Fig. 3A). **B.** Comparison of the log-transformed gene expression ratios obtained from the RNA-seq data and RT-qPCR data for the twelve selected genes by a Pearson correlation test.

Figure 5: Hierarchical clustering analysis using the TIGR MultiExperiment Viewer (MeV). Six clusters were extracted from the DEG obtained in conditions B and C (plants only aphid-infested) and F and G (plants treated with aphids and TuYV). Cluster 1 corresponds to DEG from Arabidopsis plants infested with aphids at both 6 h and 72 h, cluster 2 at only 6 h infestation, cluster 3 at only 72 h infestation. Cluster 4, 5 and 6

contain genes specifically deregulated by aphids in TuYV-infected plants at both time points (cluster 4), at 6 h (cluster 5) and at 72 h (cluster 6) respectively. DEG that were found deregulated in any other conditions (e.g. at 6 h aphid infestation and 6 h aphid and TuYV treatment) were discarded. The number of DEG in each cluster is given in brackets next to the cluster number. The log_2FC are given by shades of red and green colors according to the scale bar (red for down-regulated, green for up-regulated genes).

Figure 6: Differentially expressed genes (DEG) categorized into major Mapman bin code ontologies from *A. thaliana* infested by *M. persicae* only for 6 h or 72 h (conditions B and C, in yellow (6 h), red (72 h) and orange for the genes found at both time points, bars at the left from the separation bar) or in TuYV-infected A. *thaliana* infested by *M. persicae* for 6 h or 72 h (conditions F and G, in light and dark green respectively and intermediate green for the genes found at both time points, bars at the right from the separation bar). The scale is the same for DEG at the right and left.

Figure 7: Representation of the mRNA deregulations affecting the transcription factors (TFs) genes by clustering them into different families and according to their down or up-deregulation. The TFs were extracted from data corresponding to *A. thaliana* plants infested by *M. persicae* only for 6 h or 72 h (conditions B and C) and normalized to/with those of mock-treated plants or in TuYV-infected A. *thaliana* infested by *M. persicae* for 6 h or 72 h (conditions F and G) and normalized to those of viral-infected plants. The size of the circles is proportional to the number of deregulated TF genes (indicated in each circle).

Figure 8: Heatmap of significant relative changes in metabolite patterns in *A. thaliana* plants treated with either TuYV (A), aphids alone for 6 h (condition B) or 72 h (condition C) or both TuYV and aphids for 6 h (conditions D and F) or 72 h (conditions E and G) aphid infestation. The data were normalized to mock-treated plants as indicated below the lanes (conditions A to E), or to viral-infected plants (conditions F and G). Metabolites were grouped accordingly to their functional or chemical family as amino acids, flavonoids, glucosinolates, hormones, alkaloids, organic acids, sugars and isothiocyanates, and their specific names are given at the right. Statistical analyses were performed using the Tukey's Honest Significant Difference method followed by a false discovery rate (FDR) correction, with FDR < 0.05. For

FDR ≥ 0.05, log_2FC were set to 0. The log_2FC of significant metabolites for pairwise comparisons are given by shades of red or blue colors according to the scale bar at the right.

Supplemental data

Supplementary Table 1: Samples analyzed by transcriptomics and metabolomics. For sequencing and RT-qPCR the samples were a mixture of equal amounts of RNA extracted from individual plants. Metabolomic analysis was performed on individual plants.

Supplementary Table 2: Number of aligned reads for transcriptome profiling

Supplementary Table 3: List of primers used in real time PCR quantification (RT-qPCR) of selected genes or TuYV genome

Supplementary Table 4 : List of the 31 DEG common to plants infested by aphids for 5 or 6 h found in the data by Jaouannet et al. (2015), Bricchi et al. (2012) and ours.

Supplementary Figure S1: Venn diagram representing the overlap among DEG in the mock- and TuYV-infected plants after 6 and 72 h of aphid infestation. Green numbers indicate up-regulated DEG, red numbers indicate the down-regulated genes and the black numbers are the sum of up and down-regulated genes.

Supplementary Figure S2: Comparison of the transcriptomic data obtained in this study with data from the literature. **A.** Venn diagram illustrating the numbers of unique and common *A. thaliana* DEGs at early time of aphid infestation between Jaouannet et al. (2015) data (blue circle), Bricchi et al. (2012) (pink circle) data and our data (condition B, purple circle). Numbers in green represent up-regulated genes and those in red are down-regulated genes. Numbers at the left of the circles represent the sum of the common genes shared with our data. **B.** Venn diagram illustrating the numbers of unique and common *A. thaliana* DEGs after 72 h of aphid infestation between DeVos et al. (2005) results and ours (condition C). Below the bracket are the common genes.

Supplementary Figure S3: Gene ontology enrichment of biological processes performed on common genes identified between the data from Jaouannet et al. data (2015) (6 h), Bricchi et al. (2012) (5 h) and our early aphid infestation experiment (**A** and **B**) and those from DeVos et al. (2005) (72 h) and our late aphid infestation experiment (**C** and **D**). Down- (in red) and up-regulated (in green) genes were analyzed separately for each treatment. Gene ontology analysis was performed on DAVID functional annotation tool (https://david.ncifcrf.gov/summary.jsp). p-values are indicated for each process.

Supplementary Figure S4: Gene ontology performed on differentially expressed genes (DEG) categorized into major Mapman bin code from **(A)** *A. thaliana* infested by *M. persicae* only (6 h and 72 h grouped together) (conditions B and C) or from **(B)** TuYV-infected A. *thaliana* infested by *M. persicae* for 6 h and 72 h (grouped together) (conditions F and G). Up-regulated genes are depicted in green and down-regulated genes are in red.

Supplementary Figure S5: Clustering of mRNA deregulations of genes implicated in **(A)** hormonal responses and **(B)** genes fitting in the "protein" category. DEG were extracted from data corresponding to *A. thaliana* plants infested only by *M. persicae* for 6 h or 72 h (conditions B and C) and normalized to those of mock-treated plants or in TuYV-infected A. *thaliana* infested by *M. persicae* for 6 h or 72 h (conditions F and G) and normalized to those of viral-infected plants. Up- and down-regulated genes are grouped. The size of the circles is proportional to the number of deregulated genes (indicated in each circle).

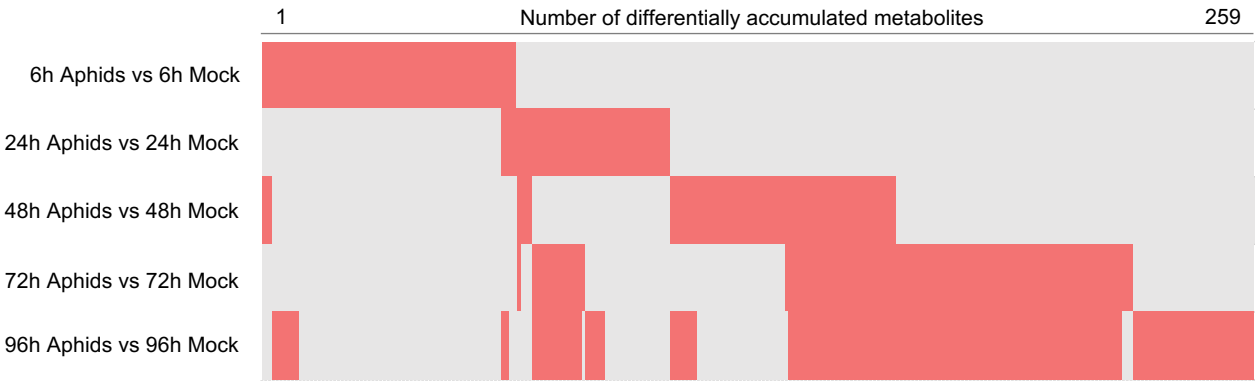

Figure 1: Time-dependent deregulations of differentially accumulated metabolites (red) in non-infected *A. thaliana* Col-0 upon aphid (*M. persicae*) infestation for 6, 24, 48, 72 and 96 h.

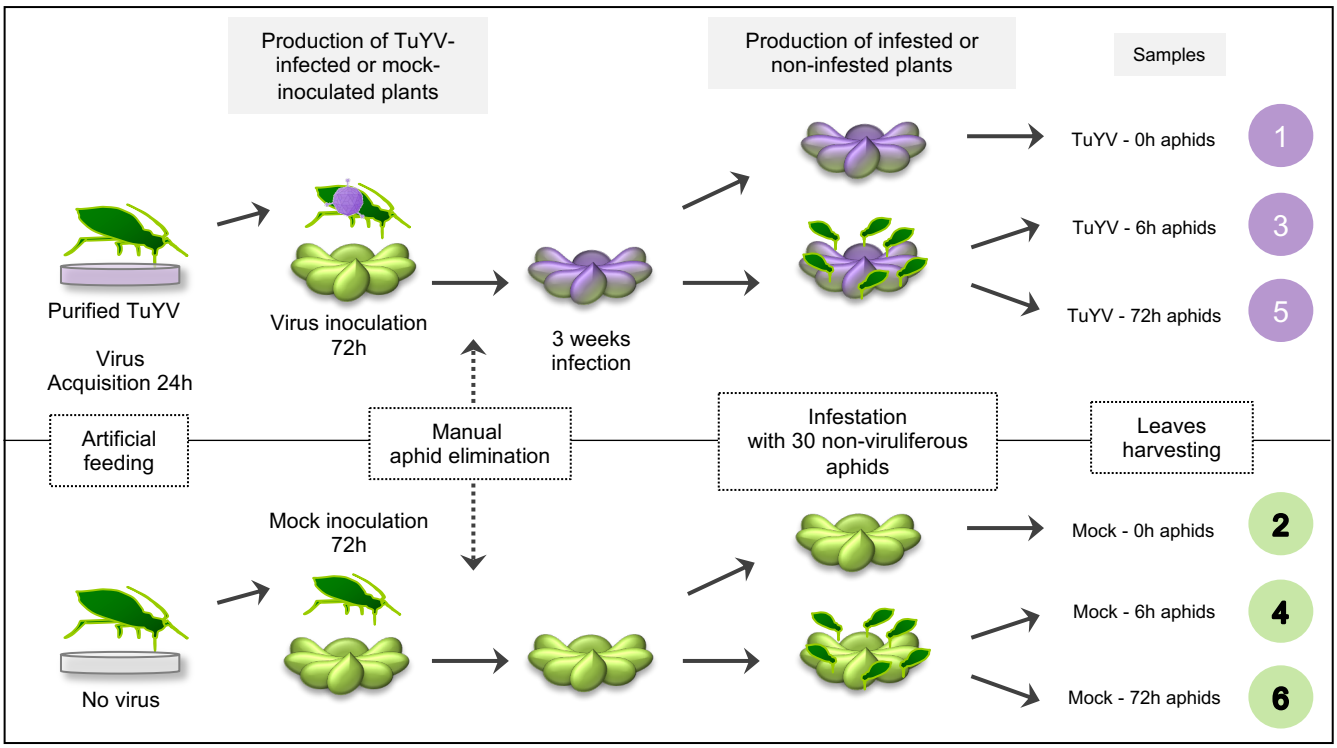

Figure 2: Experimental set-up for the high throughput transcriptomic and metabolomic analyses. Arabidopsis plants were inoculated with TuYV-viruliferous (upper panel) or non-viruliferous (lower panel) *M. persicae* aphids. After three weeks, the two batches of plants were infested with 30 non-viruliferous aphids for 6 or 72 h before harvesting (samples 3-4 and 5-6 respectively). Plants that were not infested with aphids were similarly processed (samples 1 and 2).

A

Condition	Differential analysis	Effect of
A	1 vs 2	Viral infection
B	4 vs 2	Aphids in non-infected plants at 6h infestation
C	6 vs 2	Aphids in non-infected plants at 72h infestation
D	3 vs 2	Aphids and virus in TuYV-infected plants at 6h infestation
E	5 vs 2	Aphids and virus in TuYV-infected plants at 72h infestation
F	3 vs 1	Aphids in TuYV-infected plants at 6h infestation
G	5 vs 1	Aphids in TuYV-infected plants at 72h infestation

B

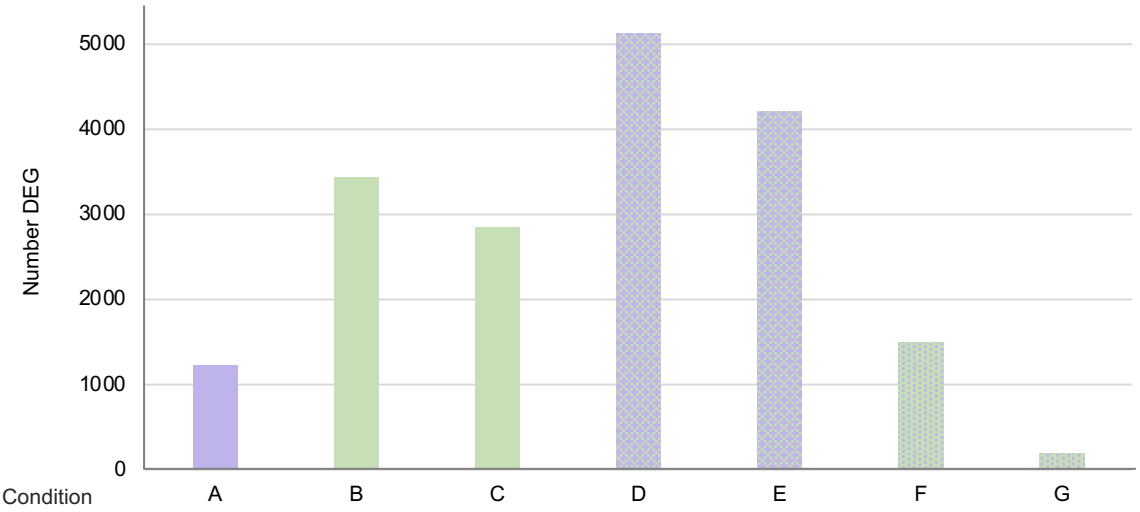

Time post-infestation	0h	6h	72h	6h	72h	6h	72h
nb DEG	1231	3434	2693	5130	4207	1490	190
up	505	1594	843	2264	1729	711	88
down	726	1840	1850	2866	2478	779	102
Differential analysis	TuYV / mock	Aphids / mock		Aphids + TuYV / mock		Aphids + TuYV/ TuYV	

Figure 3: Comparison of the number of differentially expressed genes (DEG) obtained in the various conditions. **A.** Table illustrating the seven conditions analyzed in the next figures. The data of the five samples (Fig. 2 samples 1, 3, 4, 5 and 6) were normalized to data from mock-treated plants (sample 2) or to data from virus-infected plants (sample 1), to obtain the data of the seven experimental conditions A to G. These conditions will be resumed in the high throughput transcriptomic and metabolomic analyses. **B.** Number and representation of DEG found in the seven conditions. *Arabidopsis thaliana* plants (TuYV-infected or mock-inoculated) were infested with aphids for 0, 6 or 72 h. The total number of DEG are given for each condition below the graph, with the number of up and down-regulated genes below.

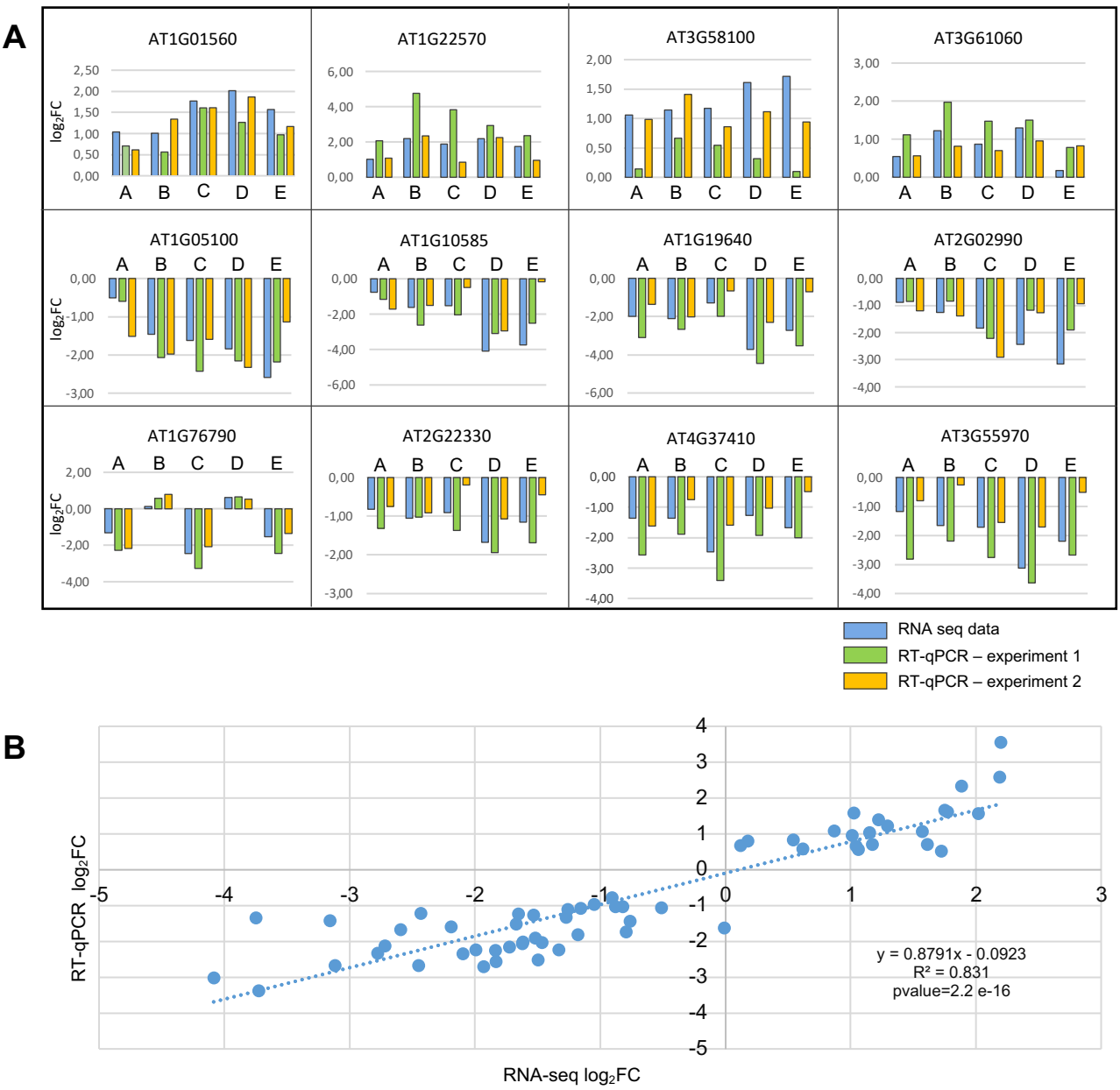

Figure 4: A. Comparison of gene expression between RNA-seq data and RT-qPCR analysis. Samples of two biological repeats were used for RT-qPCR on a subset of twelve selected genes (in green and yellow). The data obtained were normalized using data from mock-inoculated plants and the results in the form of log_2FC are presented for the conditions A to E (see Fig. 3A). **B.** Comparison of the log-transformed gene expression ratios obtained from the RNA-seq data and RT-qPCR data for the twelve selected genes by a Pearson correlation test.

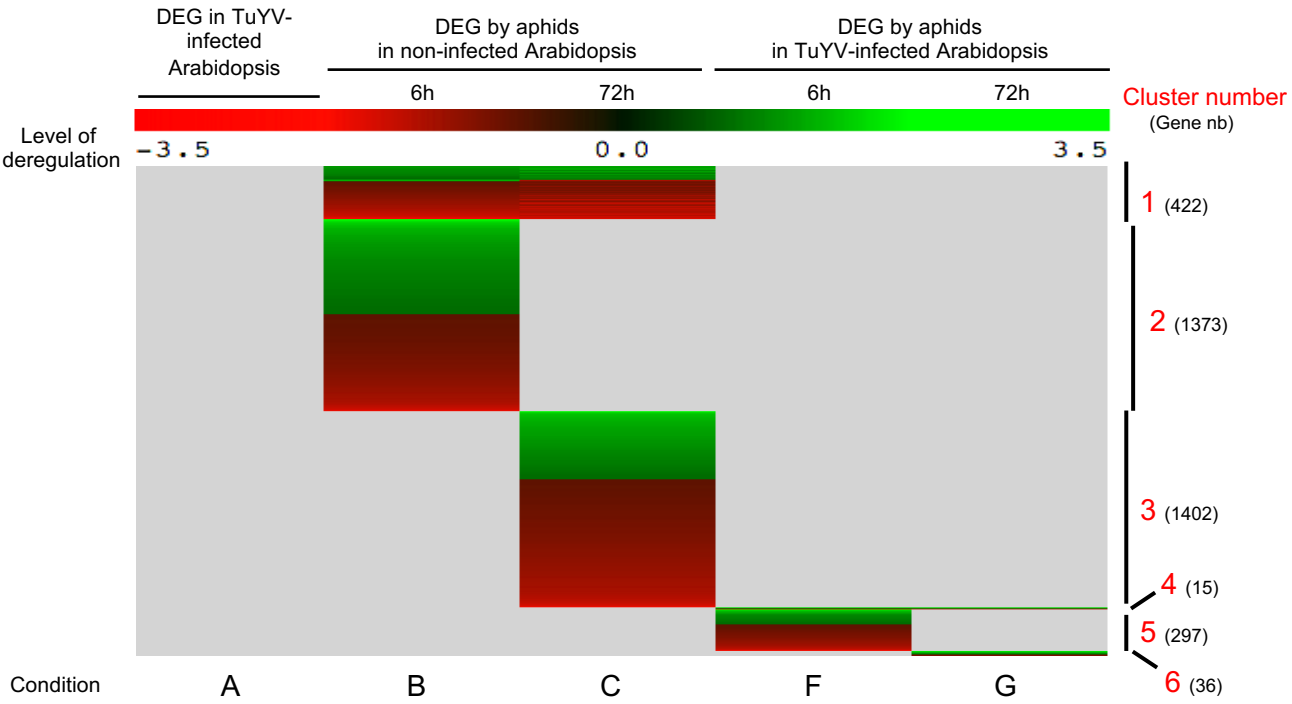

Figure 5: Hierarchical clustering analysis using the TIGR MultiExperiment Viewer (MeV). Six clusters were extracted from the DEG obtained in conditions B and C (plants only aphid-infested) and F and G (plants treated with aphids and TuYV). Cluster 1 corresponds to DEG from Arabidopsis plants infested with aphids at both 6 h and 72 h, cluster 2 at only 6 h infestation, cluster 3 at only 72 h infestation. Cluster 4, 5 and 6 contain genes specifically deregulated by aphids in TuYV-infected plants at both time points (cluster 4), at 6 h (cluster 5) and at 72 h (cluster 6) respectively. DEG that were found deregulated in any other conditions (e.g. at 6 h aphid infestation and 6 h aphid and TuYV treatment) were discarded. The number of DEG in each cluster is given in brackets next to the cluster number. The log_2FC are given by shades of red and green colors according to the scale bar (red for down-regulated, green for up-regulated genes).

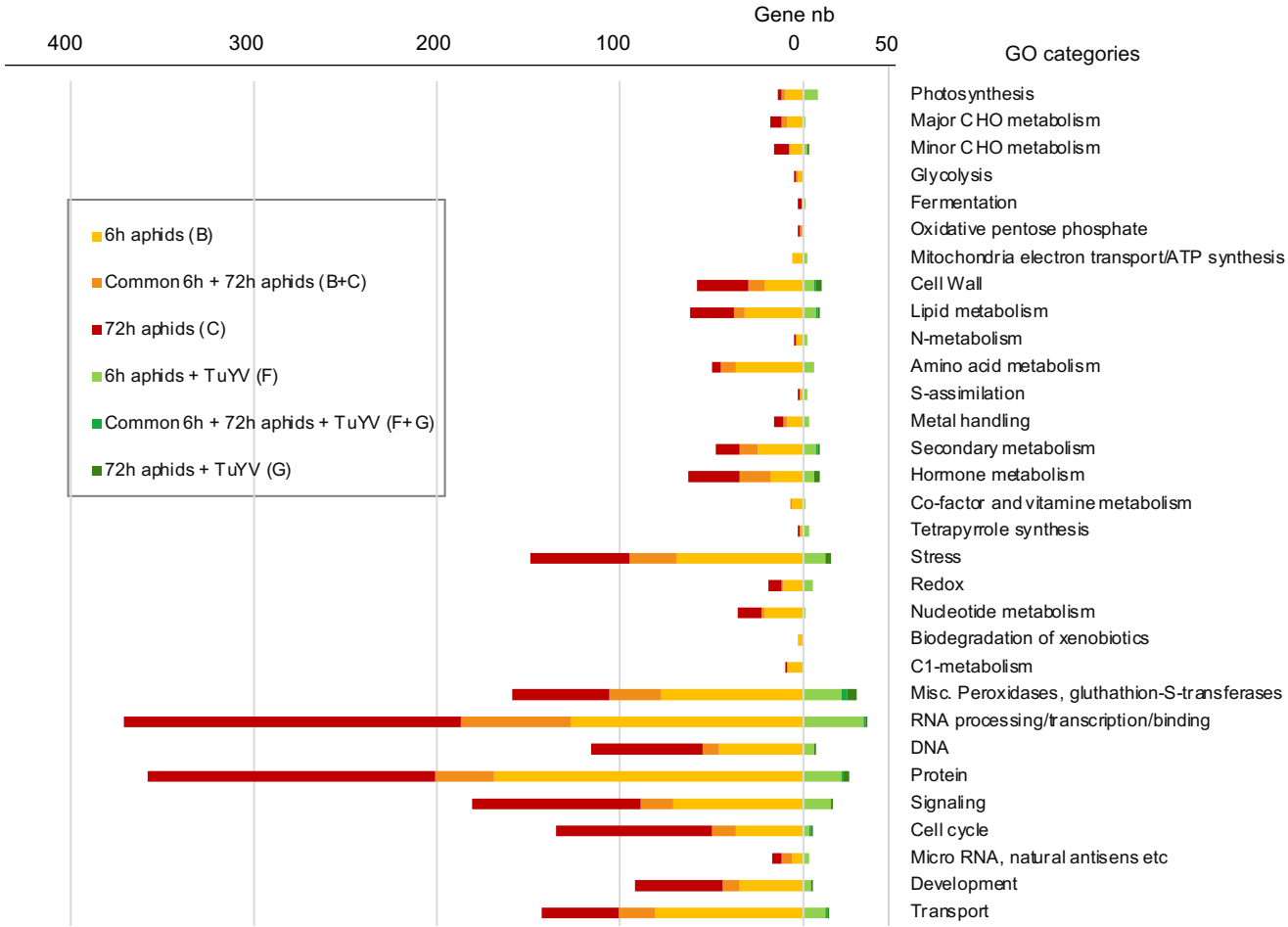

Figure 6: Differentially expressed genes (DEG) categorized into major Mapman bin code ontologies from *A. thaliana* infested by *M. persicae* only for 6 h or 72 h (conditions B and C, in yellow (6 h), red (72 h) and orange for the genes found at both time points, bars at the left from the separation bar) or in TuYV-infected A. *thaliana* infested by *M. persicae* for 6 h or 72 h (conditions F and G, in light and dark green respectively and intermediate green for the genes found at both time points, bars at the right from the separation bar). The scale is the same for DEG at the right and left.

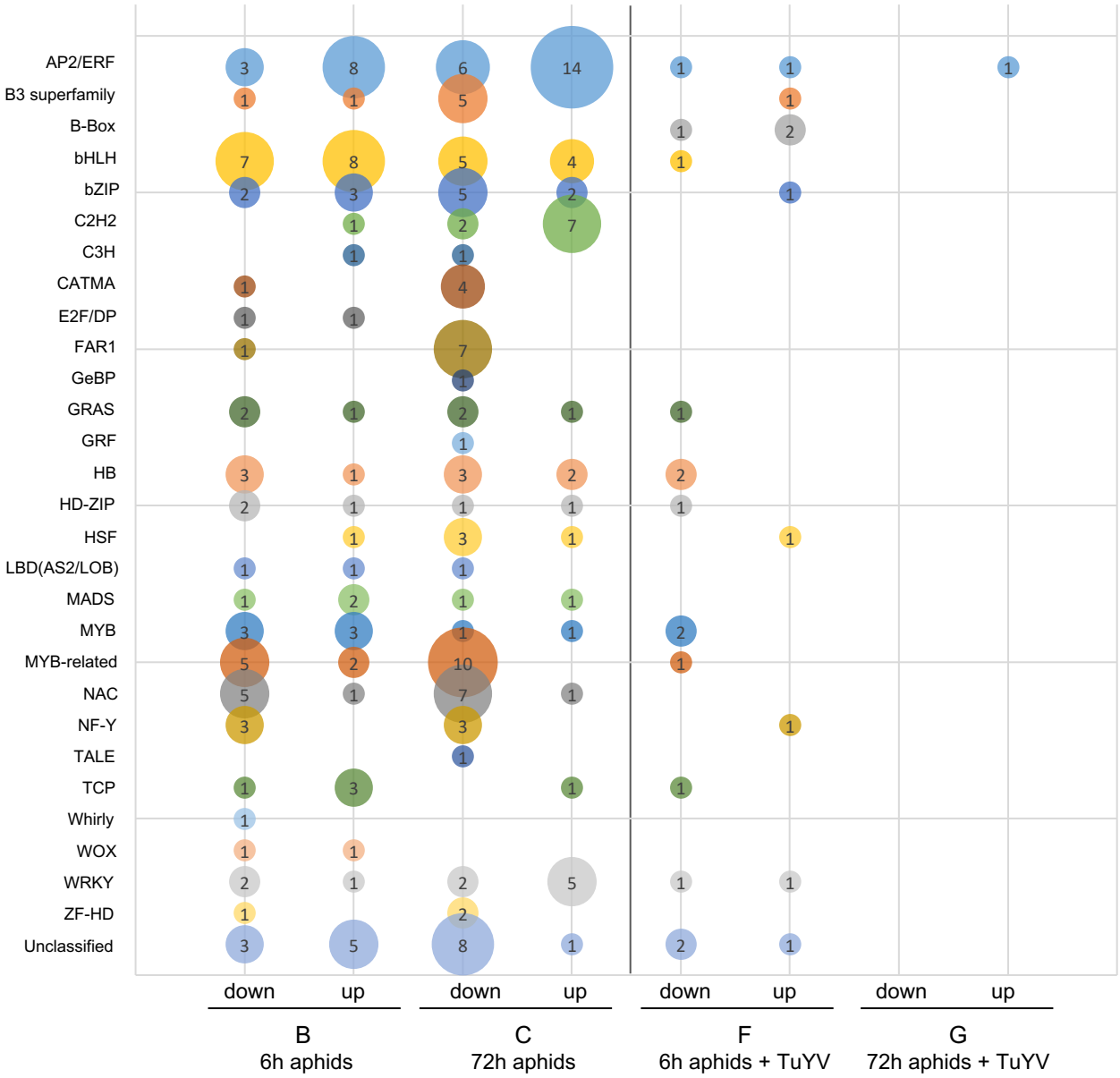

Figure 7: Representation of the mRNA deregulations affecting the transcription factors (TFs) genes by clustering them into different families and according to their down or up-deregulation. The TFs were extracted from data corresponding to *A. thaliana* plants infested by *M. persicae* only for 6 h or 72 h (conditions B and C) and normalized to/with those of mock-treated plants or in TuYV-infected A. *thaliana* infested by *M. persicae* for 6 h or 72 h (conditions F and G) and normalized to those of viral-infected plants. The size of the circles is proportional to the number of deregulated TF genes (indicated in each circle).

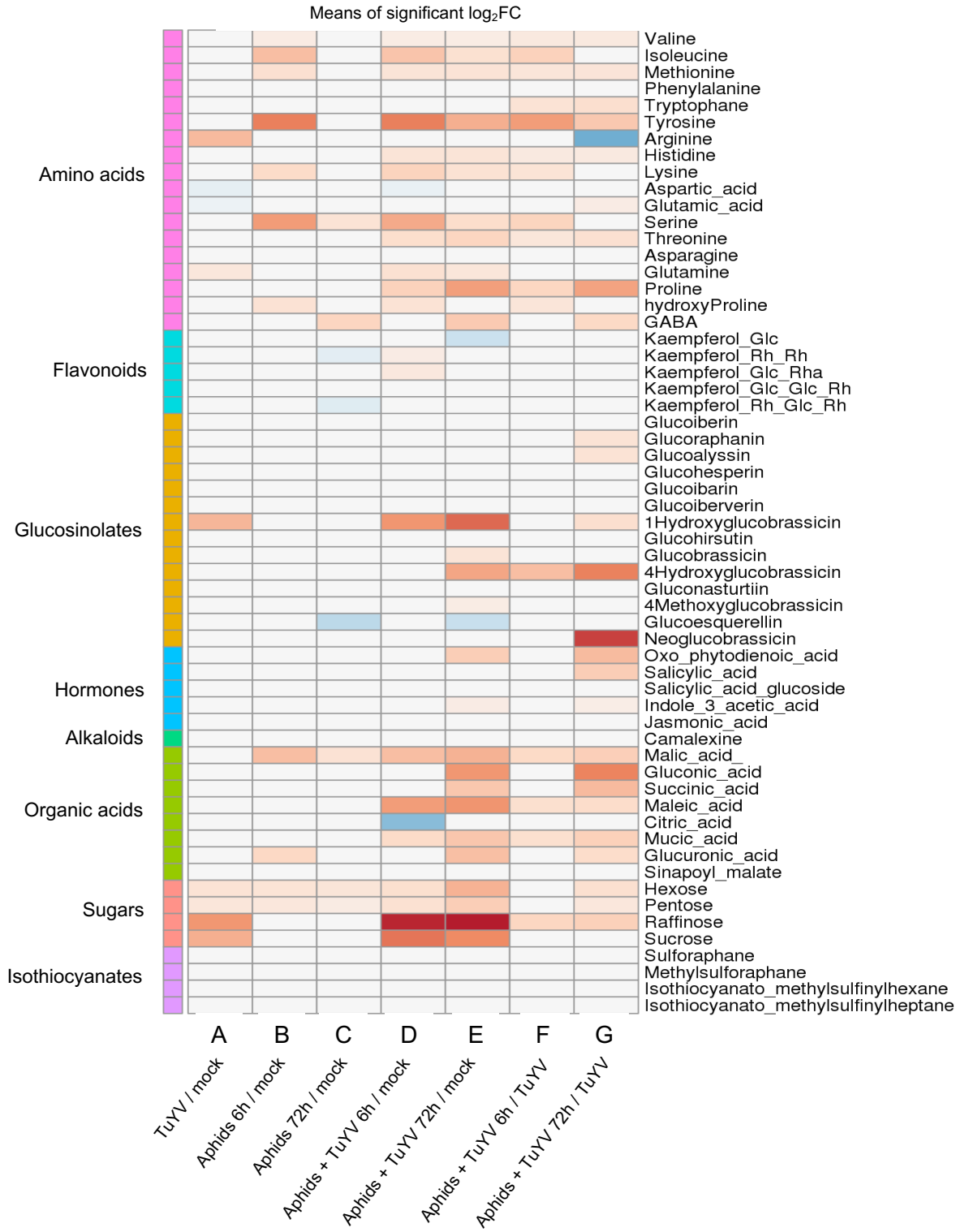

Figure 8: Heatmap of significant relative changes in metabolite patterns in *A. thaliana* plants treated with either TuYV (A), aphids alone for 6 h (condition B) or 72 h (condition C) or both TuYV and aphids for 6 h (conditions D and F) or 72 h (conditions E and G) aphid infestation. The data were normalized to mock-treated plants as indicated below the lanes (conditions A to E), or to viral-infected plants (conditions F and G). Metabolites were grouped accordingly to their functional or chemical family as amino acids, flavonoids, glucosinolates, hormones, alkaloids, organic acids, sugars and isothiocyanates, and their specific names are given at the right. Statistical analyses were performed using the Tukey's Honest Significant Difference method followed by a false discovery rate (FDR) correction, with FDR < 0.05. For FDR ≥ 0.05, log_2FC were set to 0. The log_2FC of significant metabolites for pairwise comparisons are given by shades of red or blue colors according to the scale bar at the right.

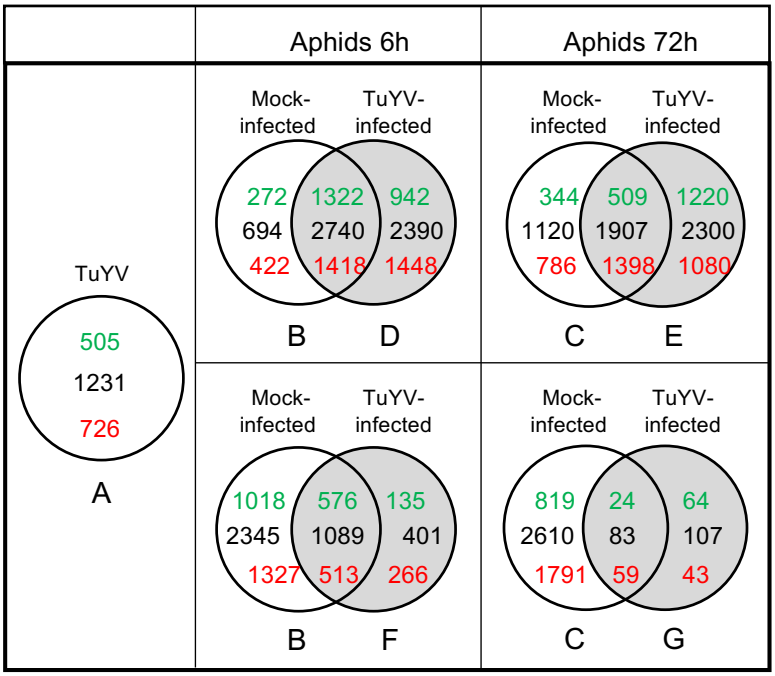

Supplementary Figure 1: Venn diagram representing the overlap among DEG in the mock- and TuYV-infected plants after 6 and 72 h of aphid infestation. Green numbers indicate up-regulated DEG, red numbers indicate the down-regulated genes and the black numbers are the sum of up and down-regulated genes.

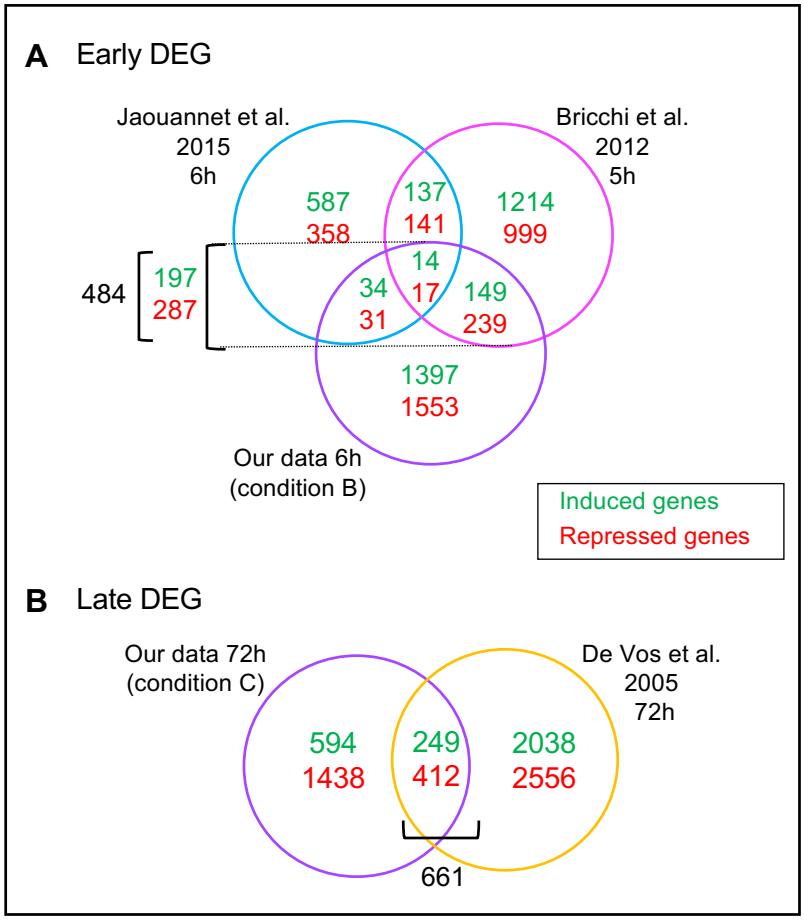

Supplementary Figure 2: Comparison of the transcriptomic data obtained in this study with data from the literature. **A.** Venn diagram illustrating the numbers of unique and common *A. thaliana* DEGs at early time of aphid infestation between Jaouannet et al. (2015) data (blue circle), Bricchi et al. (2012) (pink circle) data and our 6 h data (condition B, purple circle). Numbers in green represent up-regulated genes and those in red are down-regulated genes. Numbers at the left represent the common genes shared with our data. **B.** Venn diagram illustrating the numbers of unique and common *A. thaliana* DEGs after 72 h of aphid infestation between DeVos et al. (2005) results and ours (condition C). Below the bracket are the common genes.

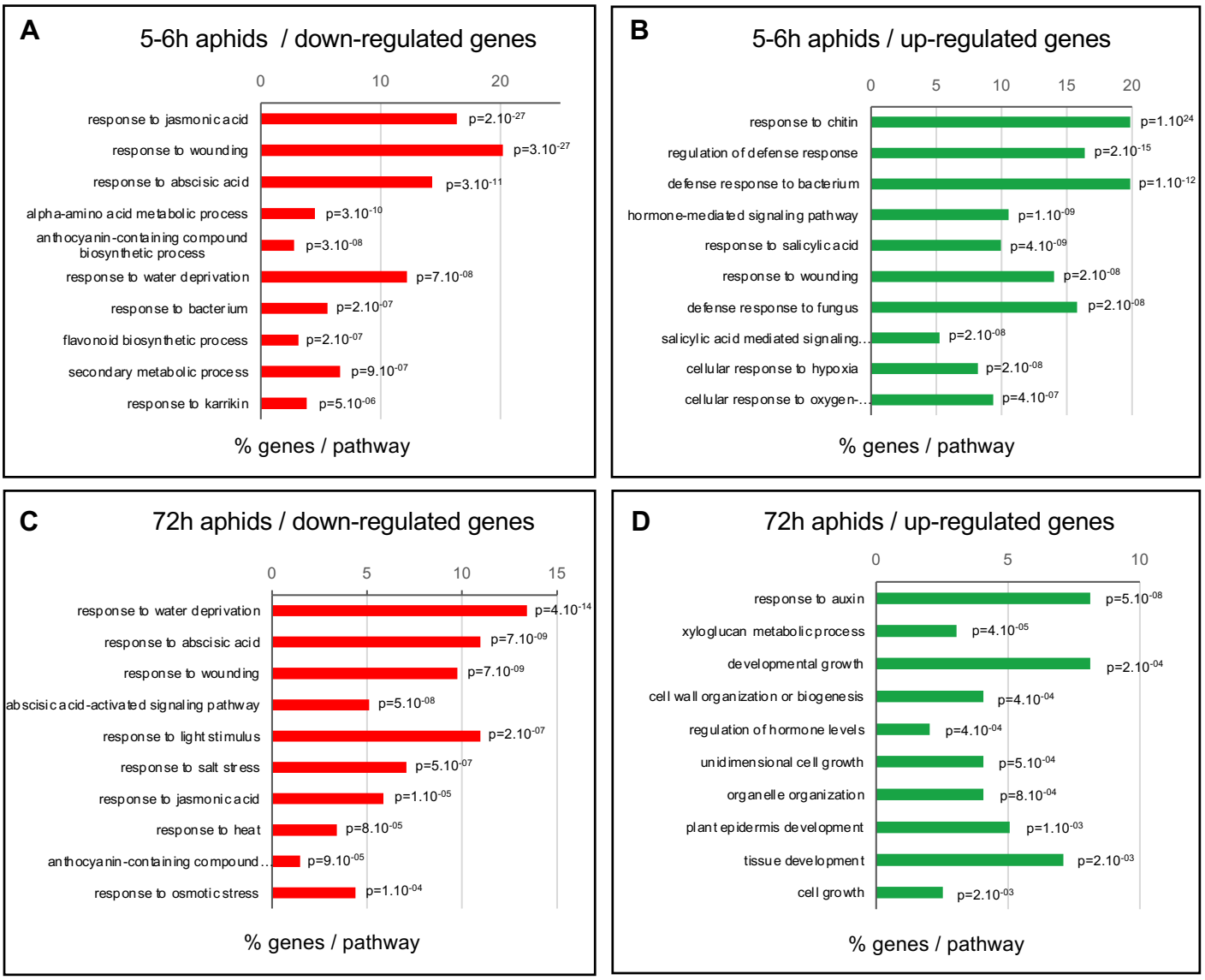

Supplementary Figure 3: Gene ontology enrichment of biological processes performed on common genes identified between the data from Jaouannet et al. data (2015) (6 h), Bricchi et al. (2012) (5 h) and our early aphid infestation experiment (**A** and **B**) and those from DeVos et al. (2005) (72 h) and our late aphid infestation experiment (**C** and **D**). Down- (in red) and up-regulated (in green) genes were analyzed separately for each treatment. Gene ontology analysis was performed on David functional annotation tool (https://david.ncifcrf.gov/summary.jsp). p-values are indicated for each process.

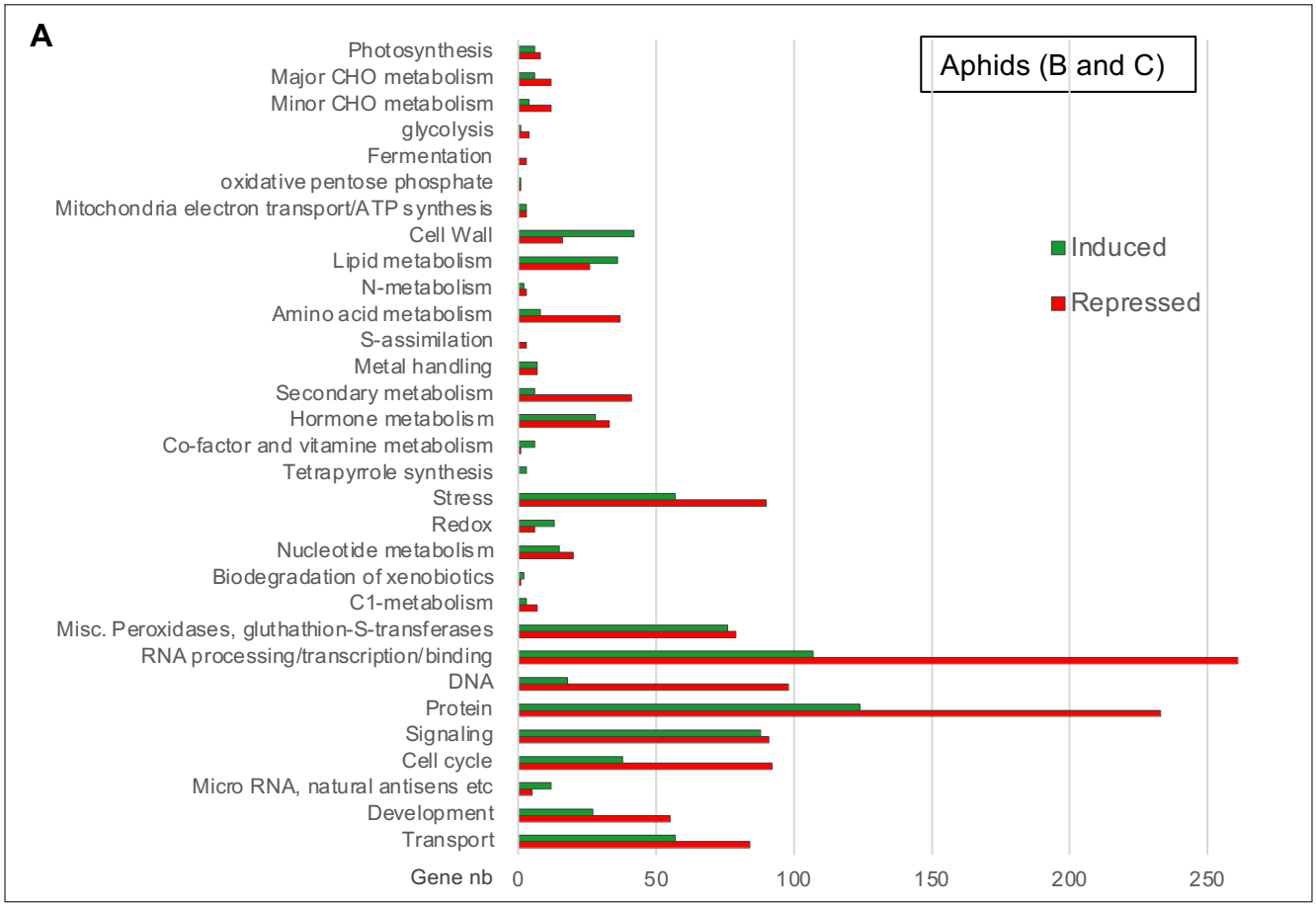

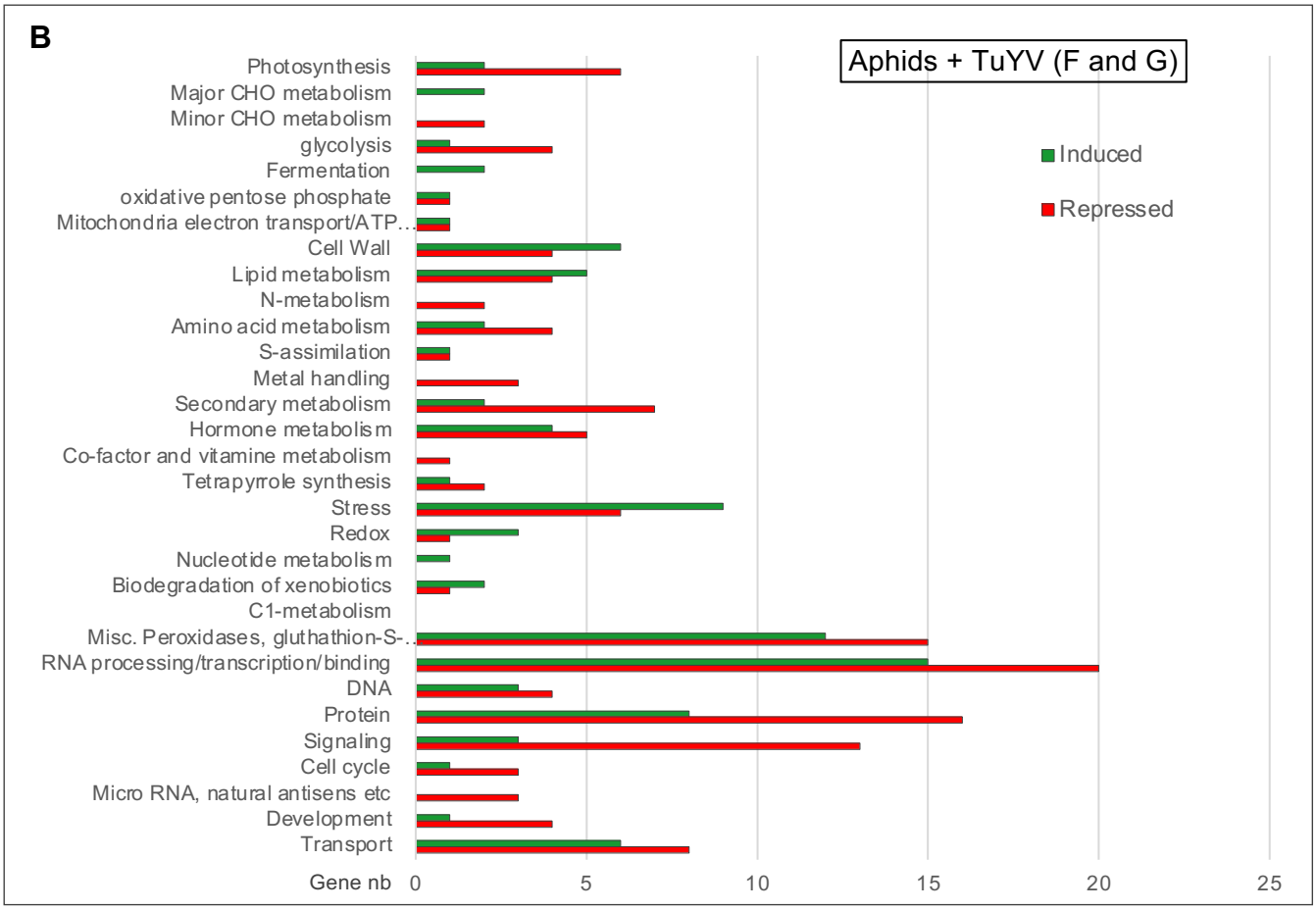

Supplementary Figure S4: Gene ontology performed on differentially expressed genes (DEG) categorized into major Mapman bin code from **(A)** *A. thaliana* infested by *M. persicae* only (6 h and 72 h grouped together) (conditions B and C) or from **(B)** TuYV-infected A. *thaliana* infested by *M. persicae* for 6 h and 72 h (grouped together) (conditions F and G). Up-regulated genes are depicted in green and the down-regulated genes are in red.

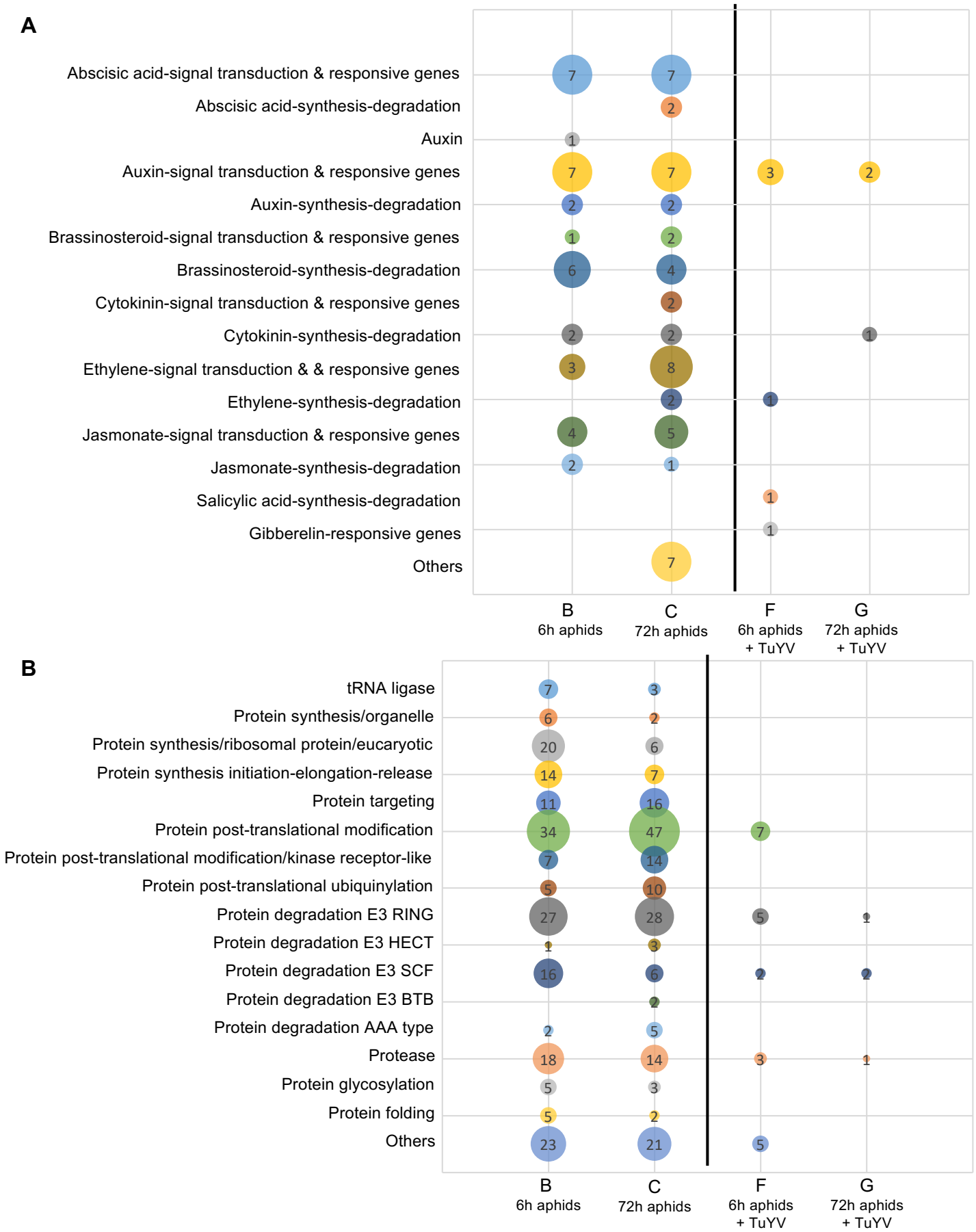

Supplementary Figure 5: Clustering of mRNA deregulations of genes implicated in **(A)** hormonal responses and **(B)** genes fitting in the "protein" category. DEG were extracted from data corresponding to *A. thaliana* plants infested only by *M. persicae* for 6 h or 72 h (conditions B and C) and normalized to/with those of mock-treated plants or in TuYV-infected A. *thaliana* infested by *M. persicae* for 6 h or 72 h (conditions F and G) and normalized to those of viral-infected plants. Up- and down-regulated genes are grouped. The size of the circles is proportional to the number of deregulated genes (indicated in each circle).